UNIVERSITY OF READING

The Shallow-Water Semi-Geostrophic Equations on the Sphere

Mark H. Mawson

A thesis submitted for the degree of Doctor of Philosophy.

Department of Mathematics

August 1994

Abstract

The semi-geostrophic equations of meteorology are considered in their shallow-water form on the sphere. To distinguish between the equations considered here and those described by Shutts and Salmon we refer to our equations as the "spherical semi-geostrophic equations". It is shown that there may exist a unique solution to these equations on the sphere for finite time under given conditions if certain key results can be proven. A robust numerical method is developed based on a finite-difference predictor/corrector scheme which uses a multigrid algorithm to solve the elliptic equation which arises in the correction step. Numerical techniques are developed which restore numerical solutions which at any stage fall outside the solution set for the equations back into it. Eulerian and semi-Lagrangian prediction schemes are compared for simulations starting from both idealised data and data tak

Acknowl dg m nts

The first, and largest, acknowledgement goes to Dr Mike Cullen for his contributions to my understanding of this work and his wealth of knowledge in both analytic and numerical techniques, and most importantly, for introducing me to this area of work in the first place. Next to Dr Mike Baines, my supervisor at Reading University, as the hour spent each Friday morning explaining things to him was usually the most useful of the week. Also for his many helpful contributions to the work, including finding all the little things I sometimes overlooked. To Dr Ray Bates for kindly supplying the semi-Lagrangian primitive equation code. To Dr Gareth Shaw for supplying the code which formed the basis of the multigrid code and for answering my questions about multigrid methods. Last,

Contents

Chapter 1

Introduction

In atmospheric modelling we are interested in predicting the motion and properties of a fluid on a sphere. For the Earth's atmosphere this is a very complicated problem with many microphysical processes interacting with the dynamical fluid motion, for example latent heating due to the c

was V. Bjerknes in the early part of this century, who recognised that there was a deterministic set of equations for the atmosphere. He also showed that the system was highly non-linear and that in general there was no analytic solution. Undaunted by this L. F. Richardson performed the first numerical weather prediction experiment, publishing his results in 1922, [59]. The calculation took several months, and unfortunately the results were found to be in error by several orders of magnitude. Perhaps because of this error, or more likely because of the time and labour involved in obtaining the results, numerical prediction remained only a hypothetical possibility until the advent of the computer. During this time the forecasters continued to use their tried and trusted methods, many of which are still commonly used today in the forecasting of phenomena, such as fog, which numerical models have yet to predict well. The techniques used by forecasters during the early part of this century are described in Shaw [67]. The first successful numerical prediction came not long after computers first appeared and was due to Charney, Fjortoft and von Neumann in 1950, [12]. Since then the rapid advances made in the power of computers have led to equally rapid growth in the complexity and size of the atmospheric models run on them. A typical operational global model in use today has a horizontal resolution of 100 kilometres and a vertical resolution of 1 kilometre, this requires around 1.2 million data points per variable held. The resolution of the model is constrained by the power of the computer and how quickly you wish to obtain the forecast from the model. To provide more detailed forecasts of what is commonly considered as weather, namely, cloud, rainfall, fog, and wind, for a particular area of the world a model with higher resolution than the global one is run for that area. Such models typically have horizontal resolutions of 30-50 kilometres and better vertical resolution in the lowest 10 kilometres of the atmosphere, of the order of 500 metres. For climate simulations, which need to be run for many decades to obtain statistically significant results, lower resolution global models are used as

scenario.

In order to improve the current numerical weather prediction models it is essential that we understand more about the real atmosphere and more about our numerical model as well. In particular, we need to understand how the model reacts to the forcing we are providing. To gain insight into how both the atmosphere and the model work much work has been done with simpler models of the atmosphere. These simpler models are usually based on equations which have had a further level of approximation made to them, and in the early days of computers were used as the basis for providing weather predictions, for example Charney et al. [12]. Much work has been done with these simpler equations confined to a plane where the Coriolis force hysab equa

fronts, see for example Holt [34], Holt and Thorpe [35], Castelli et al. [10], to list just a few. They have also been used to simulate idealised flow over a mountain, Cullen et al. [17], Pierrehumbert [58], where the topic of interest was the effect of a barrier on a uniform flow normal to it. This is of interest in the simulation of downslope wind storms where sudden strong winds and a significant rise in temperature can occur; such storms are common in mountainous areas such as the Canadian Rockies. The equations, including friction, have also been used to look at idealised sea breeze simulations, Cullen [16]. Wu and Blumen [79] have looked at the interaction between the semi-geostrophic equations and the atmospheric boundary layer as has Young [80].

We adopt a typical approach when embarking on looking at a three-dimensional problem on the sphere, and that is to first consider the shallow-water form of the equations. Instead of the full 3-d problem we now have only a 2-d one with the variation in the third direction being represented only by the changing height of the free surface. It has often been found that the major problems in a 3-d model can be found in the equivalent shallow-water problem, such as problems with the co-ordinate poles in numerical methods. Results obtained for the shallow-water problem are often readily generalised to the full 3-d one with little extra effort. We thus start by trying to prove analytically that there exists a unique solution to the semi-geostrophic shallow-water equations on the sphere, chapter 2. We then proceed to develop a robust numerical method for solving the equations, chapter 3, using some of the knowledge and insight we gained in the analytic work. This numerical method is then used to integrate forward in time both idealised and real atmospheric initial data, chapter 4. These simulations are compared with those from the shallow-water equations derived from the usual equations used in atmospheric modelling. The shallow-water simulations provide some insight into the underlying behaviour of the 3-dimensional equations but it is not expected that they will provide any significant new insight into the behaviour of

the real atmosphere. However, the results gained from the simulation of a form of Rossby-Haurwitz wave, see Haurwitz [33] for a description of the true wave, using the semi-geostrophic shallow-water equations on the sphere may do this. The extra understanding we are looking for, it is hoped, will be provided by the full 3-dimensional model. The extension of this work to 3-dimensions on the sphere is outside the scope of this thesis but some comments on this are provided in chapter 5.

We begin by stating the semi-geostrophic equations after first stating the fundamental predictive equations for the atmosphere and describing which approximations are made to obtain the usual equations used in numerical weather prediction, the so called Primitive equations.

1.1 Th s mi-g ostrophic qu tions.

Our starting point is the frictionless Navier-Stokes equations for a fluid on a rotating sphere of radius a in spherical polar co-ordinates λ, ϕ, z where $\lambda \in [0, 2\pi$, $\phi \in [\pi/2, -\pi/2]$ and z is the distance from the centre of the sphere

$$\frac{D\underline{u}_3}{Dt} = -\alpha \nabla_3 p - 2\Omega sin\phi \underline{k} \times \underline{u}_3 + \underline{g} + \nu \nabla_3^2 \underline{u}_3 \qquad 1.1$$

where α is the specific volume, Ω is the rotation rate of the sphere and the second term on the right-hand-side of the equation is known as the Coriolis term, $\underline{k}$ is the unit vector normal to the surface of the sphere, ν the viscosity coefficient and $\underline{g}$ is the gravitational force including the centrifugal forces,

$$\underline{g} = \underline{g}_a - \Omega \underline{k} \times \ \Omega \underline{k} \times \underline{r}$$

where $\underline{r}$ is the particle position measured from the origin at the sphere's centre and $\underline{g}_a$ is the gravitational force. The derivative D/Dt is the usual Lagrangian derivative and

$$\underline{u}_3 = \ u, v, w$$

$$\nabla_3 = \left(\frac{1}{a cos\phi} \frac{\partial}{\partial \lambda}, \frac{1}{a} \frac{\partial}{\partial \phi}, \frac{\partial}{\partial z} \right.$$

with ∇_3^2 the three dimensional Laplacian. We also require the conservation of mass, often refered to as the continuity equation, given by

$$\frac{1}{\alpha} \frac{D\alpha}{Dt} = \nabla_3 . \underline{u}_3 \qquad 1.2$$

We now assume that the atmosphere is a perfect gas, so that

$$p\alpha = RT \qquad 1.3$$

where T is the

and the Lagrangian derivatives are taken along the free surface. Equations 1.7 and 1.8 will be referred to the shallow-water primitive equations, and simulations with them will be used in chapter 4 as a comparison with those obtained from the semi-geostrophic equations. The simple models, which we now derive, are all based on approximations which 'balance' the horizontal pressure gradients with some function of the horizontal velocities. F

quasi-geostrophic equations are valid for a particular chosen rest state and that they cease to be so if significan

$$v = v_g + \frac{\mathcal{D}u_g}{\mathcal{D}t} - \frac{\mathcal{D}^2}{\mathcal{D}t}\left(v_g + \frac{\mathcal{D}u_g}{\mathcal{D}t}\right) + \frac{\mathcal{D}^4}{\mathcal{D}t}\left(v_g + \frac{\mathcal{D}u_g}{\mathcal{D}t}\right) - \ldots.$$

where

$$\frac{\mathcal{D}}{\mathcal{D}t} = \frac{1}{f}\frac{D}{Dt}$$

provided that

$$\left|\frac{D\underline{u}}{Dt}\right| \ll |f\underline{u}|$$

The geostrophic velocity is thus the leading order approximation to the full velocity and we adopt the notation $\underline{u_0}$ to represent the approximation of $\underline{u}$ which includes no derivative terms. In a series of papers [21], [22] Cullen and co-workers proved the existence and uniqueness of solutions to the $f-$plane semi-geostrophic equations for any finite time. The ability to prove such results is an attractive feature of this equation set and naturally poses the question as to whether the results can be extended to the semi-geostrophic equations on the sphere. The proof they obtained was constructive and formed the basis of an ingenious numerical model, the *geometric* model, Cullen and Purser [20], which is guaranteed to converge to the analytic solution of the equations as the spatial and temporal resolution is increased. A finite-difference model was then developed, Cullen [15], which could be compared with the geometric model and allowed more complicated features to be examined. If we can extend the theory to the semi-geostrophic equations on the sphere then we should be in an equally good position to construct an accurate numerical algorithm which also converges to the analytic solution. Thooarw[illegible]

1.2

at the equator where v_g is allowed to be infinite but is multiplied by $sin\phi$ which is zero. To implement this on a computer will require some very careful thought. Definitions of balance other than geostrophic can be used to define more general equation sets, such as the *linear balance equations* and the *balance equations* described in McWilliams and Gent [45]. Discussion of these equations, along with other balanced equations, can be found in that paper and in others by the same authors [30] and [31] and more recently in Allen et al. [2]. These models are more general than those derived from geostrophic balance but because they describe more atmospheric motions they may be less useful in providing the understanding that we seek. This is because their extra complexity may make it more difficult to isolate the important processes. The logical approach seems to be to extract all the understanding we can from each level of simple model and to gradually increase the models' complexity as our understanding grows. It is thus necessary that we discover what we can from models based on geostrophic balance before embarking on more complex systems.

2.1 nown r sults for th f-pl n c s

Results for the f = constant or f-plane case were prov

$$\frac{D\alpha}{Dt} = 0 \tag{2.4}$$

$$fv_0, -$$

equations can be re-interpreted as defining the motion of material parcels in the new co-ordinates. Following Cullen and Purser we call $\{\underline{X}\}$ *data space* and $\{\underline{x}\}$ *physical space*. We note that

$$\underline{U}_{\underline{X}} = \ f\ y - Y\ , f\ X - x\ , 0$$

and $\nabla_{\underline{X}}.\underline{U} = 0$ and hence equation 2.9 becomes

$$\left(\frac{\partial}{\partial t} + \underline{U}_{\underline{X}}.\nabla_{\underline{X}}\ \ \rho = 0 \right. \qquad 2.10$$

It can be shown that there exists a potential function $R\ \underline{X}$ such that $\nabla_{\underline{X}} R = \underline{x}$ and

$$R\ \underline{X}\ = f^2 \underline{x}.\underline{X} - P\ \underline{x}$$

where

$$P\ \underline{x}\ = \Phi + \frac{1}{2} f^2\ x^2 + y^2$$

and also that $\nabla_{\underline{x}} P = f^2 \underline{X}$. As pointed out by Chynoweth et al. [13] the co-ordinate transformation is simply a Legendre transform.

The solution procedure is now as follows;
Suppose that at time t we have ρ as a function of $\underline{X}$ subject to the condition that the integral of ρ over all $\underline{X}$ gives the volume of Ω in physical space. We can now solve the following Monge-Ampère equation

$$det\ \partial^2 R/\partial X_i \partial X_j\ \equiv \partial\ \nabla_{\underline{X}} R\ /\partial\ \underline{X}\ = \rho \qquad 2.11$$

to find R for the given ρ with the boundary condition that $\nabla_{\underline{X}} R = \underline{x}$ is always within Ω for all $\underline{X}$. After finding R, $\nabla_{\underline{X}} R$

not simply as advecting velocities. The constraint required to solve the system is that if the potential function P is interpreted as a surface, then it must be convex when viewed from below. This implies that R is also convex. This is equivalent to requiring general two-dimensional parcel stability for the atmospheric state as shown in Shutts and Cullen [69]. The convexity also implies that the potential vorticity q defined as $q = det\ \partial^2 P/\partial x_i \partial x_j$ is everywhere non-negative. In finite areas where the potential vorticity is zero the fields are still uniquely determined with the exception of the velocity field $\underline{u}$ which is undetermined. This is not a problem since the solution procedure does not require $\underline{u}$.

The important features of this approach can be summarized as follows;

i The co-ordinate transformation, which allows the system to be written in the simple form given by equations 2.10 and 2.11

ii The convexity of the function P, which allows the mapping between the two spaces and hence the ability to retrieve the values of all the fields from knowing just ρ.

iii The conservation law for ρ, which allows the integration to proceed for any finite time.

iv The proofs enable discontinuous solutions to be included in the theory since they require only that P and R are continuous; their derivatives need not be.

2.1.2 Application of this Procedure to the Sphere

We consider each of the important features of the approach in turn.

The co-ordinate transformation can again be applied but this now yields terms involving $\partial f/\partial y$ which cannot be absorbed into the D/Dt

since the transformation involves terms in $1/f$. Modifying the transformation to hav

2.2 Results for the equations on the sphere

We re-state the shallow-water spherical semi-geostrophic equations 1.11 - 1.14 , henceforth SSG, for ease of reference in the rest of this section.

$$\partial h/\partial t + \nabla .\ h\underline{u} \ = 0 \tag{2.12}$$

$$\partial \underline{u_0}/\partial t + \underline{u}.\nabla \underline{u_0} = -g\nabla h - f\underline{k} \times \underline{u} \tag{2.13}$$

$$g\frac{1}{acos\phi}\frac{\partial h}{\partial \lambda} - fv_0 = 0 \tag{2.14}$$

$$g\frac{1}{a}\frac{\partial h}{\partial \phi} + fu_0 = 0 \tag{2.15}$$

where $\underline{k}$ is the unit vector in the usual z direction, $f = 2\Omega sin\phi$, a is the radius of the sphere, g is the gravitational acceleration, h is the height of the free surface, $\underline{u_0} = \ u_0, v_0\ $ is the balanced wind field and $\underline{u} = \ u, v\ $ is the full wind field.

2.2.1 SSG Energy Conservation

We prove that the SSG energy defined as

$$\frac{1}{2}h\underline{u_0}^2 + \frac{1}{2}gh^2$$

is conserved when integrated over the sphere. This proof holds in fact for any closed domain with zero flow across the boundaries. A similar proof for the primitive shallow water equations can be found in Pedlosky found in itgbTj,ET,¨TD˙asT,vsphere¨TD

where we denote $\underline{u}_0.\underline{u}_0$

2.2.2 SSG Absolute Vorticity Evolution Equation

The shallow-water form of the SSG potential vorticity denoted q/f, the SSG absolute vorticity, denoted by hq/f, are defined following Hoskins [36] by

$$\begin{aligned} hq &= \left[f + \frac{1}{acos\phi}\frac{\partial}{\partial\lambda}\left(\frac{g}{afcos\phi}\frac{\partial h}{\partial\lambda}\right. - \left.\frac{gtan\phi}{a^2 f}\frac{\partial h}{\partial\phi}\right]\left[f + \frac{1}{a}\frac{\partial}{\partial\phi}\left(\frac{g}{af}\frac{\partial h}{\partial\phi}\right.\right.\right] \\ &\quad - \left[\frac{1}{a}\frac{\partial}{\partial\phi}\left(\frac{g}{afcos\phi}\frac{\partial h}{\partial\lambda}\right.\right]\left[\frac{1}{acos\phi}\frac{\partial}{\partial\lambda}\left(\frac{g}{af}\frac{\partial h}{\partial\phi}\right. + \left.\frac{gtan\phi}{a^2 fcos\phi}\frac{\partial h}{\partial\lambda}\right] \end{aligned}$$

or equivalently,

$$\begin{aligned} hq &= \left[f + \frac{1}{acos\phi}\frac{\partial v_0}{\partial\lambda} + \frac{u_0 tan\phi}{a}\right]\left[f - \frac{1}{a}\frac{\partial u_0}{\partial\phi}\right] \\ &\quad + \left[\frac{1}{a}\frac{\partial v_0}{\partial\phi}\right]\left[\frac{1}{acos\phi}\frac{\partial u_0}{\partial\lambda} - \frac{v_0 tan\phi}{a}\right] \end{aligned}$$

Here we show that the SSG equations do not have a Lagrangian conservation law for q/f. The existence of this conservation law was essential in the proof of existence and uniqueness of the f-plane semi-geostrophic equations. To do this we consider the equations on a plane in cartesian space x, y with f a function of y. We do this in cartesian co-ordinates rather than spherical polars since it simplifies the proof, as we do not have to include the metric terms, and it is easier to see which terms must cancel in order to obtain conservation of q/f on an f-plane. We wish to emphasize which terms must cancel as this cancellation will be shown to be important in making the semi-Lagrangian version of the numerical scheme work near the poles where f is nearly constant, see Chapter 3, section 3.2.2.
The definition of q in cartesian co-ordinates is

$$hq = \left(f + \frac{\partial}{\partial x}\left(\frac{g\partial h}{f\partial x}\right.\right.\left(f + \frac{\partial}{\partial y}\left(\frac{g\partial h}{f\partial y}\right.\right. - \frac{\partial}{\partial x}\left(\frac{g\partial h}{f\partial y}\right.\right.\frac{\partial}{\partial y}\left(\frac{g\partial h}{f\partial x}\right.$$

or equivalently

$$hq = \left(f + \frac{\partial v_0}{\partial x}\right.\left(f - \frac{\partial u_0}{\partial y}\right. + \left(\frac{\partial u_0}{\partial x}\right.\left(\frac{\partial v_0}{\partial y}\right.$$

and the SSG equations in cartesian co-ordinates are

$$\frac{\partial h}{\partial t} + \frac{\partial u}{\partial x} + \frac{\partial v}{\partial y} = 0$$

$$\frac{Du_0}{Dt} = -g\frac{\partial h}{\partial x} + fv$$

$$\frac{Dv_0}{Dt} = -g\frac{\partial h}{\partial y} - fu$$

$$g\frac{\partial h}{\partial x} - fv_0 = 0$$

$$g\frac{\partial h}{\partial y} + fu_0 = 0$$

where

$$\frac{D}{Dt} = \frac{\partial}{\partial t} + u\frac{\partial}{\partial x} + v\frac{\partial}{\partial y}$$

We now prove that the evolution equation for q on this cartesian plane is,

$$\frac{Dq}{Dt} = \frac{fv\beta}{h} - \frac{u\beta}{h}\frac{\partial u_0}{\partial x} - \frac{v\beta}{h}\frac{\partial u_0}{\partial y} \qquad 2.18$$

where $\beta = \partial f/\partial y$, provided that $h \in C^2$ and $u, v, u_0, v_0 \in C^1$. Where a function is in C^n if all its partial derivatives upto and including order n exist and are continuous.

The evolution equation for q/f is

$$\frac{D\ qf^{-1}}{Dt} = f^{-1}\frac{Dq}{Dt} - \beta q f^{-2} v \qquad 2.19$$

which on substituting for Dq/Dt gives a non-zero right-hand-side.

Note: If f is a constant the right-hand-sides of these evolution equations are zero and thus they become conservation laws. Thus we prove the result for the f-plane case which we stated in the previous section.

2.2.3 Existence and uniqueness of solutions on the sphere

In this section we would have liked to prove that there exists a unique solution to the SSG equations on the sphere for some finite time under certain conditions. However we have not been able to do this. We present instead an argument which would give us existence and uniqueness if the missing results can be proved. Whether these missing results can be proven is an open question. In chapter 3 we will present some numerical results which suggest that the numerical algorithm is converging to a unique solution. Although this numerical result is not a proof, it suggests that there may exist a unique solution to the SSG equations on the sphere under the conditions w

this equation is elliptic that this single equation tends to the natural boundary condition at $\phi = 0$ as we let ϕ tend to zero. This gives us an equation for the single variable at $\phi = 0$ and hence an equation for the whole sphere. We now need to prove that there exists a solution to this equation. This we are not able to do, so we state what needs to be done to prove this result. To obtain the single equation in one variable we have to assume that $\partial h/\partial t$ is continuous in time. To remove this restriction we pose a new problem and then try to prove that there exists a unique solution to this new problem. Again this has not been completed and we show what still needs to be done.

Reduction to a single equation

It is possible to reduce the system of equations 2.12 - 2.15 to one equation for the time evolution of the height field. This can be done by first using equations 2.14 and 2.15 to replace $\underline{u_0}$ in equation 2.13 provided that $f \neq 0$. This now gives equations for the time evolution of the first derivatives of the height field. The resulting equation, when written out in components, provides a pair of equations which are linear in u and v allowing us to write each of these horizontal velocity components simply in terms of the height field and its first and second derivatives. We can now replace u and v in equation 2.12 provided that q is non-zero, see section 2.2.2 for the definiton of q, to obtain the following single equation,

$$\frac{\partial h}{\partial t} + \frac{1}{a cos\phi}\frac{\partial\ hu}{\partial \lambda} + \frac{1}{a cos\phi}\frac{\partial\ hv cos\phi}{\partial \phi} = 0 \qquad 2.20$$

where

$$hu \quad = \quad \frac{1}{q}\left(-\frac{g}{a}\frac{\partial h}{\partial \phi} - \frac{\partial}{\partial t}\left(\frac{g}{af cos\phi}\frac{\partial h}{\partial \lambda} \quad \left(\frac{1}{a}\frac{\partial}{\partial \phi}\left(\frac{g}{af}\frac{\partial h}{\partial \phi} \quad + f\right.\right.\right.\right.$$

which is elliptic if

$$q > \frac{1}{4h} \; M_y - N_x \;^2 \qquad 2.22$$

Note: It is easily shown that the right-hand-side of this condition is zero if f is constant.

We have reduced the SSG equations to one equation in one unknown everywhere except $\phi = 0$. We now need to complete the reduction to one equation by finding the equation at $\phi = 0$. We note that at $\phi = 0$, $f = 0$ as well and equations 2.14 and 2.15 reduce to

$$\partial h/\partial \lambda = 0$$

$$\partial h/\partial \phi = 0$$

and differentiating with respect to t gives

$$\partial \dot{h}/\partial \lambda = 0$$

$$\partial \dot{h}/\partial \phi = 0$$

assuming that $h \in C^1$. This gives us two first order equations for $\dot{h}$ at $\phi = 0$ instead of one second order equation. We could use these equations at $\phi = 0$ along with equation 2.21 away from $\phi = 0$ and pose the question does there exist a unique solution to these equations on the sphere ? Before we contemplate this we investigate the effect that insisting equation 2.21 is elliptic has on h. Writing q in its component form equation 2.22 is

$$hq = M_x N_y - M_y N_x > \;^1$$

the *inertial stability* conditions. Inertial stability says that parcels are stable to 'small' displacements in the stated directions, in this case λ and ϕ, whilst the full criteria $q > 0$ can be considered as requiring inertial stability in all horizontal directions. It is probable that this is also a necessary condition for variable f as well. If we assume that it is then it will also be a necessary condition for equation 2.22 to be satisfied. We no

We can write μ in the general form

$$\mu = \phi^r p\ \lambda, \phi$$

for some power r and function p. Substituting this expression into the constraint on N_y to determine the restrictions on r and p gives

$$r\ r-2\ \phi^{r-3}p + \ 2r-1\ \phi^{r-2}\frac{\partial p}{\partial \phi} + \phi^{r-1}\frac{\partial^2 p}{\partial \phi^2}$$

which must tend to zero as ϕ tends to zero. This is satisfied if $r = 3+\delta$ for some $\delta > 0$ and $p \in C^2$. Thus the general form of the solution at $\phi = 0$ must be

$$h = d + c\phi^2 + \phi^{3+\delta} p\ \lambda, \phi \qquad \delta > 0 \tag{2.23}$$

where $p \in C^2$.

Substituting this general form for h in equation 2.21 and letting $\phi \to 0$ gives

$$O\ \phi^{-2}\ \left[\frac{\partial^2 \dot{h}}{\partial \lambda^2} c + \dot{p}\right] \text{Tm,TTf,gTff}$$

Proposition 2.2 *There exists a unique solution to equation* 2.21 *times* f^3 *on the sphere at time* t *if*

$$q > \frac{1}{4h} \; M_y - N_x \;^2 \geq 0 \quad \phi \neq 0$$

$$q = 0 \quad \phi = 0$$

which satisfies

$$\partial \dot{h} / \partial \lambda = 0$$

$$\partial \dot{h} / \partial \phi = 0$$

at $\phi = 0$ *with* $h \in C^n$ *on the sphere with* $n \geq 3$. *Furthermore the solution* $\dot{h} \in C^{n-1}$ *on the sphere.*

To prove this we need to know when an elliptic equation has a unique solution. The only result I have been able to find in the literature is:

Definition 2.3 *The second-order partial differential equation on a closed domain* Ω

$$\sum_{i,k=1}^{n} a_{ik} \; x_1, ..., \gamma Tc\gamma opr hTf\gamma\theta Tf\gamma TD\gamma XTTTf\gamma T\gamma\phi T\gamma Tf\gamma D\gamma T\gamma Tf\gamma TD\phi, ..., TDp\gamma m\gamma mDo\gamma\gamma Tm\gamma\tau T\gamma$$

Theorem 2.4

for which w

of the proposition, if $h \in C^n$ then $\dot{h} \in C^{n-1}$.

Finding h knowing $\dot{h}$

Assuming the existence and uniqueness of a solution to equation 2.21 , proposition 2.2, we now have an initial value problem $\dot{h} = F\ x, y, t$, where $F\ x, y, t$ is the solution of equation 2.21 . There is a unique solution to this initial value problem for t in some time interval $t_0 \leq t \leq t_1$ provided that F is continuous in this time interval and its first derivatives in space exist and are bounded. See, for example, [9], chapter 1 .

The spatial conditions on F are satisfied by our solution and it thus remains to show that F is continuous in time on this time interval. However we have already assumed this to derive equation 2.21 . We would like to remove the assumptions about continuity of h and its derivatives with respect to time. To do this we will consider the following problem,

New Problem

Given equation 2.21 on the sphere, under what conditions does it have a unique solution which is continuous in time for some time interval $[t_0, t_1]$?

We note that if its solution is continuous in time then we can go back from this equation to the SSG equations 2.12 - 2.15 , by retracing the steps used to derive this equation, and thus the conditions for the solution of this new problem are exactly those for the solution of the original one. Assuming that q is non-zero and $h \in C^3$ then the only problem in retracing the steps used to derive the single equation comes at $\phi = 0$. Here we can find the balanced velocity field, but the full velocity field is not completely determined at $\phi = 0$. To find $\underline{u}$ at the equator we can solve equation 2.12 , but this is only one equation for the two unknowns.

The velocity field $\underline{u}$ can be considered as being made up of two components, a divergent part and a rotational part. If we consider just the divergent part and substitute for $\underline{u}$ using an irrotational form in equation 2.12 then we obtain a Poisson equation. This is easily solved and thus w

The assumptions we have made guarantee a unique solution to the equation at time $t = t_b$ assuming proposition 2.2. We can form a first estimate to the solution at any other t in the interval by defining,

$$h_1\ t\ = h\ t_b\ + p\ t_b\ t$$

where $p\ t_b\ $ is the solution of our elliptic equation at time t_b. We note that by construction h is continuous on the time interval and belongs to $C^\infty\ \Omega\ $, provided that Theorem 2.4 holds for $n = \infty$ which is an open question. Assuming that the q remains bounded, inertially stable and the second partial derivatives of M, N are continuous and bounded, then we could solve the elliptic equation at a later time than t_b and hence refine our estimate. Defining $\Delta t = t_e - t_b$ we can obtain a sequence of approximations defined as follows,

$$h_m\ t\ = h\ t_b\ + \sum_{i=0}^{n-1} w_i\ t\ p_i \frac{\Delta t}{m}$$

where p_i is the solution to the elliptic equation at time $t + i\Delta t/m$ using the values of h_m at this time to calculate the coefficients and right-hand-side, and defining $t_i = t_b + \ i - 1\ \Delta t/m$ with

$$w_i\ t\ = \begin{cases} 0 & \text{if } t < t_i \\ 1 & \text{if } t > t_{i+1} \\ \ t - t_i\ /\ t_{i+1} - t_i & \text{otherwise} \end{cases}$$

It is again noted that provided each of the p_i can be found then this estimate of the solution is also continuous in time and belongs to $C^\infty\ \Omega\ $ by construction provided that Theorem 2.4 holds for $n = \infty$. We now consider what happens if we let $m \to \infty$ at time $t = t_e$.

$$h\ t_e\ = h\ t_b\ + \int_{t_b}^{t_e} p\ \tau\ d\tau$$

since $p = \dot{h}$. We noted earlier that for a unique solution to this integral equation we require that p is continuous on the time interval. We can replace the integral

by the limit of the infinite sum,

$$h\ t_e\ = h\ t_b$$

known. This single predictive equation for the Quasi-Geostrophic equations and the $f-$plane Semi-Geostrophic equations is simply a Lagrangian conservation law and is thus relatively easily solved. The recovery of the original variables from the new unknown at a later time requires the solution of an equation, a Monge-Ampère equation in the f-plane Semi-Geostrophic case, under some constraint which guarantees a unique solution. See Hoskins et al [39] for a discussion of this idea and how it might be extended to the full equations of fluid motion. We note that in their terminology the recovery of the original variables is referred to as the potential vorticity inversion and the possibility of such recovery the invertability principle. The method used for the SSG equations differs in that the evolution equation is written in terms of one of the orginal variables and so no recovery is required, unless the direct substitution used to obtain the other variables is considered as such. Effectively the two steps, prediction and recovery, used in other balanced solution procedures have been combined into one with the penalty that the evolution equation has become much more complicated.

Of interest is how large is the time interval of validity of the solution, Tw not for

2.3 Solutions b yond th br kdown

Proposition 2.5, which asserts the existence of a unique solution, is not true when q ceases to satisfy the constraint 2.22 . As stated already this could happen

since it does not allow us to change the X and Y values at a material point. This solution may also be unphysical if too large a value for ϵ is chosen. The existence of solutions at $q = 0$ allows the proof of existence of solutions for arbitrary long time via this re-arrangement idea without mixing parcel properties. To obtain a uniqueness result for the sphere a necessary first step appears to be to prove the existence of solutions on the sphere with $q = 0$ away from $f = 0$. For the $f-$plane case where $f = 0$ then the only stable solution is for h

then a global mixing type procedure. It would be desirable to find a unique way of doing this but until the theoretical results exist this is probably not possible. For typical mid-latitude values of f and realistic data the re-arrangements, although 'global' in principle, are observed from experiments with the geometric model of Cullen and Purser [20] to be confined to a small area around the points where the semi-geostrophic potential vorticity is negative. As this procedure is known to give a unique answer this seems a viable solution for such mid-latitude values. However near the equator we may need to represent the mixing process and this is typically represenrmaT,¨TD,yadiffusionoperatorwhicT,¨TD,˙Tc,hleaT,¨TD,˙Tc,afollts

rj,TD,alueysatohaeor w

unstable areas the SSG equations are inappropriate to represent such motions and the violation of the constraints is one way of diagnosing where those motions occur. Suppose we consider these equations as acting like a time lapse camera taking pictures of the atmosphere every hour or so. Then what we see as we look at the pictures at one time may be an area of instability, while the next picture shows no instability. By comparing the two we may deduce the net effect of that unstable area, and it is that net effect that we need to represent. The solution method of Cullen, for the f-plane case, allows this to be done exactly since given initial unstable data it constructs the stable minimum energy state which results. However we may wish to add extra physical understanding to this procedure. We could choose to add to our equations an extra set of physical rules, which are only active when instabilities are present and then remove those instabilities leaving us once again in a state where we can continue forward in time. This effect could be included as a forcing term on the right hand side of the equations. As the atmosphere has motions on all scales and is subject to external forcing, from solar radiation for example, such rules already exist for many processes in atmospheric prediction models and are called *Parameterization schemes*. We need to develop such schemes to represent the unstable processes found in the forced equations used here. As this is outside the scope of this work we shall not pursue this matter further. In the next chapter we only discuss how we overcame the problem of instabilities in the numerical model of the unforced equations.

2.4 Th An lytic ppro ch s Num ric l thod.

W

of equation 2.21 and solve the resulting variable coefficient elliptic problem as suggested in the outline proof of proposition 2.2. The solution to this equation can be found via a multigrid solver to be described in section 3.3. Having found this solution we multiply by our chosen timestep to find the new values of h at the next time-level. It now remains to show that these new values also satisfy

Chapter 3

Numerical solution procedure

In this chapter we describe a numerical procedure for solving the SSG equations for arbitrarily long time. The approach we used is based on a predictor/corrector method. Here we fix $\underline{u}$

3.1 Th Pr dictor/Corr ctor Appro ch

The basic idea for this method can be found in Cullen [15] where a similar approach was implemented for a 2-dimensional x, z $f-$plane version of the equations. In this section we consider whether we can prove analytically that this approach gives us a unique solution to the SSG equations. We show that for a fixed timestep Δt we can obtain a unique solution via this method if a proposition similar to 2.2 holds, but we are unable to say anything about the convergence as Δt tends to zero. However, we demonstrate, via numerical experiments, that it appears that the method convergences to the correct solution for fixed spatial resolution. We begin by re-stating the SSG equations for ease of reference.

$$\frac{\partial h}{\partial t} + \nabla . \; h\underline{u} \; = 0 \qquad 3.1$$

$$\frac{\partial \underline{u}_0}{\partial t} + \underline{u}.\nabla \underline{u}$$

then consider how these two problems may be combined to prove results for the complete system.

3.1.1 The Advection Problem

We note that equations 3.1 and 3.2 can be written in the following form;

$$M[p] \equiv \frac{\partial}{\partial t}p - \sum_{k=1}^{m} A_k\ x,t\ \frac{\partial}{\partial x_k}p - B\ x,t\ p = r\ x,t \qquad 3.5$$

where $p = p_1, ..., p_n$ is a vector with each p_k a function of $x = x_1, ..., x_m$ and t, $A_k\ x,t$ are Hermitian matrices of degree n. For equation 3.1 $n = 1$ since there is only one variable h, while for equation 3.2 , $n = 2$ since there are tw

Proof:

3.1.2 The Correction Problem

We require that at any given time t_1 equations 3.3 and 3.4 are satisfied. Given any $\underline{u_0}\ x, y, t_1$ and $h\ x, y, t_1$ this will generally not be true and we obtain instead non-zero residuals on the right hand sides.

Question: Do there exist conditions on the given data such that there exists a unique vector $\underline{u^A}\ x, y$ which re-arranges the given data such that equations 3.3 and 3.4 are satisfied ?

Denoting the solution by $\underline{u_0^A}$,h^A, we construct the desired vector $\underline{u^A}$ as an instantaneous velocity which corrects the given data $\underline{u_0}$ and h using the SSG advection equations 3.1 and 3.2 giving

$$u_0^A = u_0 - \frac{u^A}{acos\phi}\frac{\partial u_0}{\partial \lambda} - \frac{v^A}{a}\frac{\partial u_0}{\partial \phi} + \frac{u^A v_0 tan\phi}{a} - \frac{g}{acos\phi}\frac{\partial\ h^A - h}{\partial \lambda} + fv^A \qquad 3.6$$

$$v_0^A = v_0 - \frac{u^A}{acos\phi}\frac{\partial v_0}{\partial \lambda} - v^{AA}$$

The choice of forward Euler is the simplest and gives the simplest form for the resulting correction equation.

If we denote by Δ the difference between the solution and the given data then we can obtain from equations 3.3 and 3.4 the following corrector equations,

$$\frac{g}{acos\phi}\frac{\partial \Delta h}{\partial \lambda} - f\Delta v_0 = -R_{ew} \qquad 3.9$$

$$\frac{g}{a}\frac{\partial \Delta h}{\partial \phi} + f\Delta u_0 = -R_{ns} \qquad 3.10$$

where R_{ew} and R_{ns} are the residuals of equations 3.3 and 3.4 for the given data.

We can replace the Δ quantities in these equations by using equations 3.6 and 3.8 to leave two equations in the unknown velocity $\underline{u^A}$.

$$\frac{g}{acos\phi}\frac{\partial D}{\partial \lambda} - f\left(f + \frac{1}{acos\phi}\frac{\partial v_0}{\partial \lambda} + \frac{u_0 tan\phi}{a}\right) u^A - \frac{f}{a}\frac{\partial v_0}{\partial \phi}v^A + \frac{fg}{a}\frac{\partial D}{\partial \phi} = R_{ew} \qquad 3.11$$

$$\frac{g}{a}\frac{\partial D}{\partial \phi} + f\left(\frac{1}{acos\phi}\frac{\partial u_0}{\partial \lambda} - \frac{v_0 tan\phi}{a}\right) u^A - f\left(f - \frac{1}{a}\frac{\partial u_0}{\partial \phi}\right) v^A - \frac{fg}{acos\phi}\frac{\partial D}{\partial \lambda} = R_{ns} \qquad 3.12$$

where we have defined $D = \nabla . h\underline{u^A}$. It now possible to use equation 3.11 to substitute for u^A in equation 3.12 provided that the terms multiplying u^A are non-zero. Similarly we can use equation 3.12 to substitute for v^A in equation 3.11 provided that the terms multiplying v^A are non-zero. Under these assumptions we have

$$\left(f - \frac{1}{a}\frac{\partial u_0}{\partial \phi} + \frac{f}{a}\frac{\partial v_0}{\partial \phi}\right)\left(\frac{g}{acos\phi}\frac{\partial D}{\partial \lambda} - fqhu^A\right) + \left(f^2 - \frac{f}{a}\frac{\partial u_0}{\partial \phi} - \frac{1}{a}\frac{\partial v_0}{\partial \phi}\right)\left(\frac{g}{a}\frac{\partial D}{\partial \phi}\right.$$
$$= \left(f - \frac{1}{a}\frac{\partial u_0}{\partial \phi}\right)R_{ew} - \frac{1}{a}\frac{\partial v_0}{\partial \phi}R_{ns} \qquad 3.13$$

$$g\left(f + \frac{1}{acos\phi}\frac{\partial v_0}{\partial \lambda} + \frac{u_0 tan\phi}{a} + \frac{f}{acos\phi}\frac{\partial u_0}{\partial \lambda} - \frac{fv_0 tan\phi}{a}\right)\frac{\partial D}{\partial y} - fqhv^A$$

$$-g\left(f^2+\frac{f}{a\cos\phi}\frac{\partial v_0}{\partial\lambda}+\frac{fu_0\tan\phi}{a}-\frac{1}{a\cos\phi}\frac{\partial u_0}{\partial\lambda}+\frac{v_0\tan\phi}{a}\right.\quad\frac{\partial D}{\partial x}$$

$$=\left(f+\frac{1}{a\cos\phi}\frac{\partial v_0}{\partial\lambda}+\frac{u_0\tan\phi}{a}\right.\quad R_{ns}+\frac{1}{a\cos\phi}\frac{\partial u_0}{\partial\lambda}-\frac{v_0\tan\phi}{a}R_{ew}\qquad 3.14$$

If $f\neq 0$ and $q\neq 0$ see section 2.2.2 for the definition of q , we can multiply both equations 3.13 and 3.14 by $1/fq$. If we take the divergence of the resulting equations, namely

$\nabla.\quad 3.13\ /fq,\ \ 3.14\ /fq\ ,$

we obtain one equation for D of the following form,

$$\frac{1}{a\cos\phi}\frac{\partial}{\partial\lambda}\left(\frac{A}{a\cos\phi}\frac{\partial D}{\partial\lambda}\right.\quad+\frac{1}{a\cos\phi}\frac{\partial}{\partial\lambda}\left(\frac{B_1}{a}\frac{\partial D}{\partial\phi}\right.$$

$$+\frac{1}{a\cos\phi}\frac{\partial}{\partial\phi}\left(\frac{B_2}{a}\frac{\partial D}{\partial\lambda}\right.\quad+\frac{1}{a\cos\phi}\frac{\partial}{\partial\phi}\left(\frac{C\cos\phi}{a}\frac{\partial D}{\partial\phi}\right.$$

$$-D=RHS\qquad 3.15$$

where A,B_1,B_2,C are functions of f,h,and first derivatives of $\underline{u_0}$ and RHS is a function of f,h,R_{ew},R_{ns} and first derivatives of $\underline{u_0}$.

The condition for this equation to be elliptic is,

$$q\ 1+f^2\ >\frac{1}{4h}\nabla.\underline{u_0}\left(\nabla.\underline{u_0}-2f\left(f+\frac{1}{a\cos\phi}\frac{\partial v_0}{\partial\lambda}+\frac{u_0\tan\phi}{a}\right.\quad-2f\left(f-\frac{1}{a}\frac{\partial u_0}{\partial\phi}\right.$$

Equation 3.15 is similar to equation 2.21 and to complete equation 3.15 on the =

$$\frac{\partial D}{\partial \phi} = 0$$

$\forall \lambda$ at $\phi = 0$. Multiplying equation 3.15 by $fq^{\,2}$ and expanding the coefficients proves that equation 3.15 becomes $\partial D/\partial \phi = 0$ as $\phi \to 0$. If proposition 2.2 can be proven then a similar argument could be used to prove existence and uniqueness for equation 3.15 .

This unique D determines, via equations 3.11 and 3.12 a unique $\underline{u^A}$.
We can now use equations 3.6 - 3.8 to obtain the solution $\underline{u_0^A}, h^A$ which satisfies

Define

$$\underline{u}\ \lambda, \phi, t\ = \underline{u}\ \lambda, \phi, t_0\ + \underline{u^A}\ \lambda, \phi$$

$q \neq 0$ which we have already assumed, and hence they must also converge. Given that we do not know A, to prove convergence it is sufficient to show that the sequence is a Cauchy sequence, i.e.

given $\epsilon > 0$ there exists N such that $\forall m, n > N$,

$$|A_n - A_m| < \epsilon$$

Since $\Delta t_n \to 0$ as $n \to \infty$ it is sufficient to show that,

$$|A_n - A_m| < M|\Delta t_n - \Delta t_m|$$

for some bounded constant M.

W

in Section 3.1.4. If the advection equations were simply conservation laws of the form

$$\frac{\partial W}{\partial t} + \nabla \ uW$$

where W represents any of the variables h, u_0 or v_0, and the residuals did not contain derivatives, then it would be possible to show that $R \to 0$ as Δt tends to zero for a simple time-marching algorithm eg: forward Euler. This result is independent of the actual function $\underline{u}$. As the choice of $\underline{u}$ obviously changes the solution, this choice of $\underline{u}$ is important. Thus to prove $R \to 0$ as Δt tends to zero it is necessary to bound the right-hand-side of the advection equations with the time truncation error. I do not believe this can be done without knowledge of the function $\underline{u}$.

3.1.4 Convergence Results derived from Numerical Experiments

A numerical version of the predictor/corrector method was implemented as described in section 3.2. The numerical results given here are for the Heun local-timestepping advection scheme, see section 3.2.2 for details, with two iterations of the corrector step. Similar results are obtained with the other advection schemes.

Convergence to a unique solution

We choose a fixed resolution of 192 by 129 points and take for our initial data real 500hpa fields valid at 2.00 GMT on the 1st February 1991 which we shall call time t_0. We choose time t_1 to be 3.04 GMT on the same day and obtain the fields valid at this time via the numerical method with a particular choice of the

timestep. We calculate E_{jk}, M_{jk}, E^{∞}_{jk} and M^{∞}_{jk} defined as follows,

$$E_{jk} = \frac{1}{N}\sum_{i=1}^{N} |h\ \lambda_i, \phi_i, t_1, \Delta t_j\ - h\ \lambda_i, \phi_i, t_1, \Delta t_k\ |$$

$$M_{jk} = E_{jk}/|\Delta t_j - \Delta t_k|$$

$$E^{\infty}_{jk} = \max_{1\le i\le N} |h\ \lambda_i, \phi_i, t_1, \Delta t_j\ - h\ \lambda_i, \phi_i, t_1, \Delta t_k\ |$$

$$M^{\infty}_{jk} = E^{\infty}_{jk}/|\Delta t_j - \Delta t_k|$$

where i loops over all N points in the domain, and Δt_j, Δt_k divide $t_1 - t_0$ exactly. E_{jk} is the left-hand-side of our Cauchy inequality, except that it is the L_1 mean over all points, E^{∞}_{jk} is the largest value in the domain which typically occurs at the same point for all choices of Δt. M_{jk} and M^{∞}_{jk} are the constants on the right-hand-side of the inequalities which we wish to bound to show convergence.

Note: For this time period the special steps taken to enforce the required constaints on the data to ensure solutions exist were not required for any of the timesteps.

We choose $\Delta t_1 = 1$ minute. All timesteps in the table are in minutes.

j	Δt_j	E_{1j}	M_{1j}	E^{∞}_{1j}	M^{∞}_{1j}
2	2	1.69138×10^{-3}	1.69138×10^{-3}	4.42710×10^{-2}	4.42710×10^{-2}
3	4	5.07192×10^{-3}	1.69063×10^{-3}	0.13299	4.43294×10^{-2}
4	8	1.18311×10^{-2}	1.69015×10^{-3}	0.31020	4.43139×10^{-2}
5	16	2.53300×10^{-2}	1.68867×10^{-3}	0.66529	4.43525×10^{-2}
6	32	5.22773×10^{-2}	1.68644×10^{-3}	1.37714	4.44241×10^{-2}
7	64	1.06399×10^{-1}	1.68887×10^{-3}	2.80488	4.45220×10^{-2}

The same approach was applied to initial data from 20.00 GMT on the 4th June 1992 giving the following results,

j	Δt_j	E_{1j}	M_{1j}	E^{∞}_{1j}	M^{∞}_{1j}
2	2	1.69287×10^{-3}	1.69287×10^{-3}	4.43717×10^{-2}	4.43717×10^{-2}
3	4	5.07752×10^{-3}	1.69251×10^{-3}	0.13309	4.43639×10^{-2}
4	8	1.18414×10^{-2}	1.69163×10^{-3}	0.31079	4.43999×10^{-2}
5	16	2.53515×10^{-2}	1.69010×10^{-3}	0.66672	4.44477×10^{-2}
6	32	5.23244×10^{-2}	1.68789×10^{-3}	1.38166	4.45697×10^{-2}
7	64	1.06575×10^{-1}	1.69167×10^{-3}	2.82161	4.47875×10^{-2}

Thus it appears that for these two cases that

$$E_{1j} = M|\Delta t_1 - \Delta t_j|$$

and

$$E^{\infty}_{1j} = M^{\infty}|\Delta t_1 - \Delta t_j|$$

where $M = sup\ M_{1j}$ and $M^{\infty} = sup\ M^{\infty}_{1j}$ are bounded, in fact almost constant. Since we cannot run exhaustively all initial data with all timesteps we can never make a definitive statement about numerical convergence. However from these two, randomly chosen, general data cases the results suggest that the method conveTj4“–wm“TTD4–umtannot–“,s–wTD4–MTj4u“TD4–makTj“– –T“ET4q4c4lt coT“Ij4u“TD4

Convergence of the residuals

For the case of the 4th June 1992 the quantity

$$R_j = \sum_{i=1}^{N} \sum_{n=1}^{(t_1 - t_0)/\Delta t_j} |R_{ew}|_n + |R_{ns}|_n \ \Delta t_j$$

was calculated, where N is the number of grid-points in the domain. The calculations were performed for the same time period and timesteps as Section 3.1.4. Assuming $R \to 0$ as $\Delta t \to 0$ then we can write

$$R = c\Delta t^n$$

in time as the timestep tes tno–imezero.the–result–tes tgained–the–herimeho

and in spherical polars

$$\delta\ h\ \lambda,\phi\ = \frac{1}{a\Delta\lambda cos\phi}\ h\ \lambda+\Delta\lambda/2,\phi\ - h\ \lambda-\Delta\lambda/2,\phi$$

$$\delta_\phi h\ \lambda,\phi\ = \frac{1}{a\Delta\phi}\ h\ \lambda,\phi+\Delta\phi/2\ - h\ \lambda,\phi-\Delta\phi/2$$

$$\delta_{\phi c} h\ \lambda,\phi\ = \frac{1}{a\Delta\phi cos\phi}\ h\ \lambda,\phi+\Delta\phi/2\ cos\ \phi+\Delta\phi/2\ -h\ \lambda,\phi-\Delta\phi/2\ cos\ \phi-\Delta\phi/2$$

$$\overline{h\ \lambda,\phi\ }\ =\ h\ \lambda+\Delta\lambda/2,\phi\ + h\ \lambda-\Delta\lambda/2,\phi\ \ /2$$

$$\overline{h\ \lambda,\phi\ }^{\phi} =\ h\ \lambda,\phi+\Delta\phi/2\ + h\ \lambda,\phi-\Delta\phi/2\ \ /2$$

We also define

$$\underline{U} =\ U,V\ =\ uh,vh$$

and

$$h\ x,y,t+n\Delta t\ = h^n\ x,y$$

or simply h^n, with $h^n\ \lambda,\phi\ $ defined analogously. We note that

$$\overline{\overline{h}^x}^y = \overline{\overline{h}^y}^x = \overline{h}^{xy}$$

and that this holds for λ and ϕ also.

3.2.1 Computational Grid Choices

We have chosen to use a finite difference model on a uniformly spaced grid in $\lambda,\phi\ $ space. This has the disadvantage of creating problems at the poles of the sphere where we need to hold n polar values for each row, given that we have n points on a row. This is not a serious problem for scalar quantities, such as the height of the free surface h, where all the values are the same but care must be taken with the vector quantities $\underline{u_0}$ and $\underline{u}$. In this section we consider the arrangement of the variables on the computational grid and how this affects the accuracy of the discretised equations, as well as identifying any spurious solutions generated by a pn

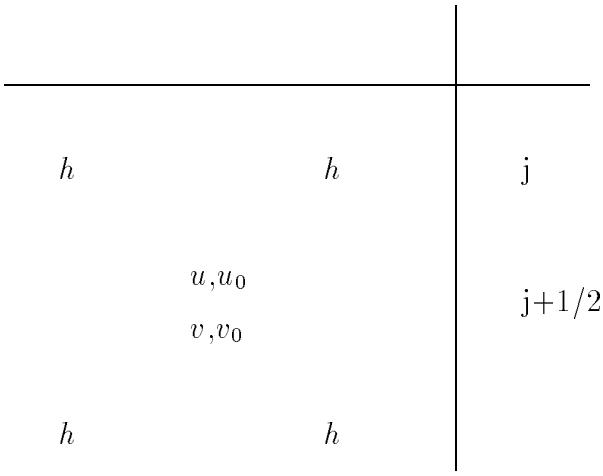
h
h
j
u,u0
v,v0
j+1/2
h
h

h		h	
h	u,v	h	

exact. This procedure, as for the C-grid, needs iterating and because of the smoothing of the height field update, it typically takes many iterations to converge to the same accuracy as the C-grid solution obtains without iteration. To derive the same accuracy as the C-grid procedure involves at least an order of magnitude more iterations and this is computationally very expensive. This inability to remove the residuals efficiently along with the computational chequerboard mode has convinced us that we should not solve the equations on the B-grid.

So far we have not considered the effect of the grid choice on which variables are held at the poles and on the equator. We consider just the C-grid since we have discarded the B-grid. In the last chapter we required $\partial h/\partial t$

$$u_{0c}^{np} = \frac{1}{n}\sum_{i=1}^{n} \left[\right.$$

For small values of $\Delta\phi$ we have $sin\ \Delta\phi/2\ = \Delta\phi/2$ to a good approximation, O $\Delta\phi/2\ ^3$, and hence the area is approximately

$$\Delta\phi\Delta\lambda cos\phi,$$

and so the cosine which represents the area is almost exactly the analytic value of the cosine at the mid-point of the grid box. If we evaluate this integral at the pole we find that the cosine value which represents the area is $cos\ \pm\pi/2 \mp \Delta\phi/4$ to the same degree of approximation. This is the value that we need to use at the poles and not the analytic value of zero.

3.2.2 Prediction Schemes

We consider two different numerical schemes for the prediction of h and $\underline{u_0}$ at time $t + \Delta t$ given $h, \underline{u_0}$ and $\underline{u}$ at time t. The first is an explicit *Eulerian* advection scheme which has been used for many years and is currently the basis of the U.K. Meteorological Office operational numerical weather prediction model. The second is a *semi-Lagrangian* scheme which has been successfully applied to the primitive equations by many authors, for example McDonald and Bates [44], and shown to have some advantages over standard Eulerian schemes. We wish to see if there is any benefit in applying the semi-Lagrangian approach to the SSG equations. In this section w

–Hu“TD4–hemeD4–advTmerical““TD4–tions h

scheme and investigate its temporal accuracy we consider just the simple advection equation,

$$\frac{\partial h}{\partial t} = -c\frac{\partial h}{\partial x} \qquad 3.18$$

The first step of the Heun advection scheme is to form a first approximation of h^{n+1}, denoted $h^{\#}$

of x and t, as is the case for the general advection equations we are using in the SSG model, then the scheme is still first order accurate and tends to second order accuracy as c tends to a constant.

Spatial Accuracy

If we use centred finite differences then we obtain second order spatial accuracy. If higher order accuracy is required it can be achieved simply by broadening the stencil to include more points and using standard higher order centred approximations to the derivatives. In this section we limit ourselves to second order accuracy for simplicity. See Cullen and Davies [18] for an example of a fourth accurate scheme.

Von Neumann Stability

We consider the Heun scheme applied to our simple advection problem 3.18 and we define a wave solution $h^n = \Lambda^n$

a

acsxi.““–to““TD4eeT–a1Neumannpcj4a

with

$$|\Lambda|^2 = 1 - \ kc\Delta$$

equation.

The discretised momentum equations consist of an advective part and two forcing

$$u_0^{n+1} = H\ u_0^n\ - \Delta t\ g\delta\ \overline{h}^{\phi} - fV/\overline{h}^{\phi}$$

$$v_0^{n+1} = H\ v_0^n\ - \Delta t\ g\delta_{\phi}\overline{h}\ + fU/\overline{h}$$

where $H\ u_0^n$ represents the Heun advection of u_0^n given at each step by

$$u_0^{\#} = u_0^n - \overline{\left(\overline{\left(\frac{U}{\overline{h}}\right)}^{\phi}\ \delta\ u_0^n\right)}\ - \frac{V}{\overline{h}^{\phi}}\delta_{2\phi}u_0^n + \overline{\left(\frac{U}{\overline{h}}v_0^n\right)}^{\phi}\frac{tan\phi}{a}$$

and $H\ v_0^n$ represents the Heun advection of v_0^n given at each step by

$$v_0^{\#} = v_0^n - \frac{U}{\overline{h}}\delta_2\ v_0^n - \overline{\left(\overline{\left(\frac{V}{\overline{h}^{\phi}}\right)}\ \delta_{\phi}v_0^n\right)}^{\phi}\ - \frac{U}{\overline{h}}\overline{u_0^n}^{\phi}\frac{tan\phi}{a}$$

The choice of averaging of the trigonometric terms involving $tan\phi$ which arise from the co-ordinate transformation is arbitrary and the one shown here is certainly not the only choice. It is, perhaps, the most natural choice and experiments with other averagings did not demonstrate any significant sensitivity to the choice. The accuracy properties of the discretisation are not affected by the co-ordinate transformation, which just leaves the question of stability. The Von Neumann stability analysis performed previously requires the ratio of Δx to Δy to remain fixed which is not true in spherical geometry. Therefore we cannot perform the analysis and hence we cannot investigate the choice of the averaging of the trigonometric terms on stability. Again experiments have shown little sensitivity to the choice. Assuming that the linear analysis would hav

i) Local Time-stepping.

The idea is to choose a timestep Δt which gives a stable prediction scheme at low latitudes and then perform multiple applications of the advection step with a correspondingly shorter, and hence stable, timestep at higher latitudes. Each of these adv

remove this restriction were not made since it was seen from experiments that multiple applications of the Heun scheme in the $\lambda-$direction only w

on a row, such that the following is satisfied

$$\max |u\ \lambda, \phi\ | \frac{\Delta t}{a \Delta \lambda cos \phi} sin\ k \Delta \lambda\ < 1$$

If $k = n/2$ than there are no unstable waves on that row. Experiments have shown that it is beneficial to insist that no row polewards of another can have more stable waves then that row. For each row with unstable waves we perform a discrete fast Fourier transform, often abbreviated to fft, to obtain the real and imaginary Fourier coefficients for each wave-number. We now damp the unstable waves by setting

$$r_j^d = r_j \left(\frac{k}{j} \right)^2 \quad k < j \leq \frac{n}{2}$$

where k is the maximum stable wave number, j is the wave number we wish to damp and r_j and r_j^d represent the undamped and damped Fourier coefficient respectively. Both real and imaginary coefficients are damped equally. We now perform another fast Fourier transform to return the damped wave representation to grid-point values. The choice of damping function is empirical and we have chosen the one used in the U.K. Meteorological Office unified model, see Cullen et al [19].

The equations at the poles and the equator

In spherical geometry we need to define what we mean by the equations at the poles. The mass equation becomes,

$$h^{np} = -D^{np} = -\sum \delta_{\phi c} V = \sum \frac{1}{cos^{np} \phi} V\ \lambda, \pi/2 - \Delta\phi/2\ cos\ \pi/2 - \Delta\phi/2$$

$$h^{sp} = -D^{sp} = -\sum \delta_{\phi c} V = -\sum \frac{1}{cos^{sp} \phi} V\ \lambda, -\pi/2 + \Delta\phi/2\ cos\ -\pi/2 + \Delta\phi/2$$

where the superscripts np and sp denote the values at the north and south poles respectively. The U term does not appear since the integral of $\delta\ U$ around a row

is identically zero. For the momentum equations we need only consider u_0 since we defined v_0 at the poles and equator in section 3.2.1. On the u_0 row next to the pole we need to define U at the pole to use in the calculation of $\overline{U}^{\phi}$; we set U at the pole to zero. For the rows half a grid-length either side of the equator we have to form $\overline{U}^{\phi}$ and so we require U on the equator and this is not well defined. We therefore define U on these rows to be the value of U on the row half a grid-length polewards of this row. This choice gives a significant reduction in numerical noise near the equator when compared to using the value of U at the equator in forming U half a grid-length either side of the equator. We note that across the equator the inertial stability code, to be described in section 3.2.3, and used to enforce ellipticity and hence the existence of a solution, ensures that

$$u_0\ \lambda, \Delta\phi/2\ = u_0\ \lambda, -\Delta\phi/2\ \ \forall\lambda$$

which has the effect of removing the cross equatorial advection of u_0 since $V\delta_{\phi}u_0$ is identically zero across the equator.

B. The Semi-Lagrangian Scheme

Consider the forced advection equation for some scalar P

$$\frac{DP}{Dt} = F\ \ P, x, y, t$$

where x and y are space variables, t is time and F some known forcing function. Given this equation at time t_0 the solution at time t_1 can be obtained via a *Lagrangian* approach as

$$P_a = P_d + \int_d^a F$$

where subscript a denotes the value at the arrival point at time t_1, d the value at the departure poin

the arrival points will generally hav

estimate of $\underline{u}_m$. This is done by solving the iterative equations

$$\underline{u}_m^n \; t + \Delta t/2 \; = \underline{u} \; x_a - u_m^{n-1}\Delta t/\Delta x, y_a - v_m^{n-1}\Delta t/\Delta y, t + \Delta t/2$$

where superscript n denotes the nth iterate and the first guess is obtained by extrapolating $\underline{u}$ at time t at the arrival points to time $t + \Delta t/2$ using a second order accurate extrapolation. For example,

$$\underline{u} \; t + \Delta t/2 \; = \; 3/2 \; \underline{u} \; t \; - \; 1/2 \; \underline{u} \; t - \Delta t$$

which gives a second order accurate temporal approximation to the departure point. In practice McDonald [42] found that a single iteration with a bi-linear interpolation to obtain the value at the mid-point was sufficient, with more iterations and higher order interpolation yielding no noticeable benefit. In chapter 4 we shall use both first and second order accurate trajectory routines.

Interpolation

The spatial accuracy of the advective part of the scheme is determined by the accuracy of the interpolation of the quantity at the departure point. The spatial truncation error is found to be one order higher than the order of the interpolation so that, for example, cubic interpolation gives a fourth order accurate scheme, see for example Staniforth and Côté [72]. A second order accurate scheme can be obtained by linear interpolation but many authors, eg McDonald [42], have found such sc

This just leaves the forcing term to consider. A second order temporal accurate approximation to the forcing term is given by the trapezium rule

$$F\ t+\Delta t\ +F\ t\ /2$$

and thus the whole scheme is second order accurate in time, fourth order in space.

Implementation in the SSG model

The mass equation written in Lagrangian form is

$$\frac{Dh}{Dt} = -h\nabla.\underline{u}$$

which becomes

$$h_a = h_d - \Delta t\ \nabla.\underline{U}_d\ t\ +\nabla.\underline{U}_a\ t+\Delta t\ /2$$

when discretised using a semi-Lagrangian approach and the trapezium rule. The first problem is that we do not know $\underline{U}$ at $t+\Delta t$ and we cannot calculate it until after the correction step. An alternative second order accurate form is to use the mid-point rule to obtain

$$h_a = h_d - \Delta t\nabla.\underline{U}_m\ t+\Delta t/2$$

where we could find $\underline{U}$ at the mid-point using the same calculation that we used to find $\underline{u}$ for the calculation of the departure point. The more significant problem is the same as when we considered using the Heun scheme to solve this equation and is the inconsistency introduced between how the equation is solved in the corrector and predictor steps. This inconsistency, as noted earlier, can lead to large errors near the equator where only $\nabla.\underline{U}$ is well defined and $\underline{u}$ is not. We therefore use the Eulerian form of the mass equation exactly as we did in the Heun scheme

$$h_a\ t+\Delta t\ =$$

and this gives only first order accuracy in time, second order accuracy in space. For momentum we adopt the vector approach of McDonald and Bates [44] as described in Bates et al. [7]. We write the equation in its vector form

$$\frac{D\underline{\underline{u_0}}}{Dt} = -g\nabla h - f\underline{k} \times \underline{\hat{u}}$$

where $\underline{k}$ is the usual unit vector in the direction normal to the surface of the sphere and

$$\underline{\hat{u}} = \left(\frac{U}{\overline{h}}, \frac{V}{\overline{h}^{\phi}} \right.$$

This can be discretised as

$$\begin{aligned} \underline{\underline{u_0}}_a &= \underline{\underline{u_0}}_d - \frac{\Delta t}{2} [\ g\nabla h_d\ t\ +\ f\underline{k} \times \underline{\hat{u}}\ t\ _d \\ &\quad +\ g\nabla h_a\ t + \Delta t\ +\ f\underline{k} \times \underline{\hat{u}}\ t + \Delta t\ _a\ ] \end{aligned} \qquad 3.22$$

to give second order accurate solutions in space and time. The vector approach

ectoras
h

the balanced velocit

$\underline{u_0}$ and here we consider how we might do this. In section 2.3 we identified two processes which apply in the $f-$plane case for $f \neq 0$ and $f = 0$ respectively. In the first case the solution can always be found by re-arranging the fluid to satisfy the constraint and in the second the only solution is $h = constant$ which can be obtained by uniformly mixing all the fluid. In the numerical code we must ensure that the partial differential equation to be solved in the correction step is elliptic, and this is the analogue of the existence conditions for the theoretical problem. We approximate the first process by simply re-arranging the balanced velocities to satisfy the inertial stability conditions. The conditions are

$$f\ f + \delta\ v_0 + u_0 tan\phi/a\ > 0 \qquad 3.25$$

$$f\ f - \delta_\phi u_0\ > 0 \qquad 3.26$$

We note that the first condition depends on u_0 whilst the second is independent of v_0. W

the iteration near the equator. If, on iteration r, no updates are performed then the condition is enforced. A solution always exists since u_0 set to the global mean of the input values at the start of the routine, satisfies the algorithm. This routine mimics a simple arrangement of the parcels by swapping values whilst also including some smoothing which is comparable to the mixing process required in the $f = 0$ case.

The first condition can be enforced on each row as it has no global dependence, unlike the u_0 condition where the mean value at the equator couples all the columns together. We set v_0 at the equator to zero and then at each point on the other rows we form

$$E = f \quad f + \delta \; v_0^n + u_0 tan\phi/a$$

where u_0 is the value obtained after enforcing the second inertial stability condition, 3.26 . If $E \leq 0$ at some point λ, ϕ we form the updates

$$v_0^{n+1} \; \lambda + \Delta\lambda/2, \phi \; = v_0^n \; \lambda + \Delta\lambda/2, \phi \; - \alpha E/f + m$$

$$v_0^{n+1} \; \lambda - \Delta\lambda/2, \phi \; = v_0^n \; \lambda - \Delta\lambda/2, \phi \; + \alpha E/f - m$$

where α and m have the same values as before. A solution always exists provided that $u_0 tan\phi/a$ is not significantly greater than f, which is the case only for non-physical flows by which time the solution is meaningless.

In the development of the code the inability to remove inertial instability was the usual sign that the code was failing and this was used to determine when the procedure should be stopped. Enforcing inertial stability is not sufficient to guarantee existence of the solutions, see Shutts and Cullen [69], for the exact conditions. Instead we require that q is greater than some positive, data dependent, value which, as we shall see in the next section, is sufficient to guarantee ellipticity of the reduced elliptic equation 3.37 . However, solving the reduced equation with inertial stability enforced and the full ellipticity condition not satisfied is found to still lead to the generation of spurious solutions. We must therefore find

a way of ensuring that the full condition is satisfied. It has not been possible to find a 2-D finite difference discretisation that mimics the $f-$plane re-arrangement procedure performed by the geometric model of Cullen and Purser [21], *Cullen personal communication* . We therefore implement a global mixing procedure which is done using a diffusion scheme. This scheme is applied to $\tilde{q} = hq$ rather than q as it is computationally cheaper to implement and numerical experiments showed that it had no detrimental impact. The first step is to form $\tilde{q}$ and then solve the following conservative diffusion equation for the increments $\Delta\tilde{q}$

$$\Delta\tilde{q} = \frac{1}{acos\phi}\frac{\partial}{\partial\lambda}\left(\frac{C}{acos\phi}\frac{\partial\tilde{q}}{\partial\lambda}\right. + \frac{1}{a}\frac{\partial}{\partial\phi}\left(C_\phi\frac{1}{a}\frac{\partial\tilde{q}}{\partial\phi}\right.$$

where we have to specify the coefficients C and C_ϕ. We wish to diffuse $\tilde{q}$ only in the areas where it is likely to violate the ellipticity conditions and so we choose to specify the coefficients dependent on the current value of $\tilde{q}$ relative to the value $\tilde{q}$ would have if there was no flow, namely f^2. We first note that the maximum stable diffusion coefficients given by linear stability analysis are

$$C^{max}\ \phi\ = \frac{1}{4}\frac{a\Delta\lambda cos\phi\ ^2}{\Delta t}$$

$$C_\phi^{max} = \frac{1}{4}\frac{a\Delta\phi\ ^2}{\Delta t}$$

where the $\lambda-$direction coefficient depends on the latitude ϕ. We now define the $\tilde{q}$ dependent coefficients at a point λ, ϕ as

$$C\ \ \lambda, \phi\ = \begin{cases} 0 & \text{if } \tilde{q} > \alpha f^2 \\ C^{max}\ \phi\ \times\ \alpha f^{23236q} & \end{cases}$$

where α and β are parameters which control the switching on of the diffusion and the point below which the maximum stable value should be used. In practice we found that

$$\alpha = .25,\ \beta = .15$$

gave good results for all the cases considered in the next chapter. We now need to find the implied increments to the height field given by the diffusive correction $\Delta\tilde{q}$ since we can then find the corresponding increments to $\underline{u_0}$ via the balance equations. We need to solve

$$\begin{aligned}
&\left[f + \frac{1}{a\cos\phi}\frac{\partial}{\partial\lambda}\left(\frac{g}{af\cos\phi}\frac{\partial\ h+\Delta h}{\partial\lambda} - \frac{g\tan\phi}{a^2 f}\frac{\partial\ h+\Delta h}{\partial\phi}\right]\right. \\
&\qquad\left[f + \frac{1}{a}\frac{\partial}{\partial\phi}\left(\frac{g}{af}\frac{\partial\ h+\Delta h}{\partial\phi}\right.\right] \\
&\qquad - \left[\frac{1}{a}\frac{\partial}{\partial\phi}\left(\frac{g}{af\cos\phi}\frac{\partial\ h+\Delta h}{\partial\lambda}\right.\right] \\
&\left[\frac{1}{a\cos\phi}\frac{\partial}{\partial\lambda}\left(\frac{g}{af}\frac{\partial\ h+\Delta h}{\partial\phi} + \frac{g\tan\phi}{a^2 f\cos\phi}\frac{\partial\ h+\Delta h}{\partial\lambda}\right]\right. &= \tilde{q} + \Delta\tilde{q}
\end{aligned}$$

This simplifies to

$$\begin{aligned}
&\left[\frac{1}{a\cos\phi}\frac{\partial}{\partial\lambda}\left(\frac{g}{af\cos\phi}\frac{\partial\ \Delta h}{\partial\lambda} - \frac{g\tan\phi}{a^2 f}\frac{\partial\ \Delta h}{\partial\phi}\right]\left[\frac{1}{a}\frac{\partial}{\partial\phi}\left(\frac{g}{af}\frac{\partial\ \Delta h}{\partial\phi}\right.\right.\right. \\
&- \left[\frac{1}{a}\frac{\partial}{\partial\phi}\left(\frac{g}{af\cos\phi}\frac{\partial\ \Delta h}{\partial\lambda}\right.\right]\left[\frac{1}{a\cos\phi}\frac{\partial}{\partial\lambda}\left(\frac{g}{af}\frac{\partial\ \Delta h}{\partial\phi} + \frac{g\tan\phi}{a^2 f\cos\phi}\frac{\partial\ \Delta h}{\partial\lambda}\right]\right. \\
&\qquad + M_x\left[\frac{1}{a}\frac{\partial}{\partial\phi}\left(\frac{g}{af}\frac{\partial\ \Delta h}{\partial\phi}\right.\right] \\
&\qquad + N_y\left[\frac{1}{a\cos\phi}\frac{\partial}{\partial\lambda}\left(\frac{g}{af\cos\phi}\frac{\partial\ \Delta h}{\partial\lambda} - \frac{g\tan\phi}{a^2 f}\frac{\partial\ \Delta h}{\partial\phi}\right]\right. \\
&\qquad - M_y\left[\frac{1}{a\cos\phi}\frac{\partial}{\partial\lambda}\left(\frac{g}{af}\frac{\partial\ \Delta h}{\partial\phi} + \frac{g\tan\phi}{a^2 f\cos\phi}\frac{\partial\ \Delta h}{\partial\lambda}\right]\right. \\
&\qquad - N_x\left[\frac{1}{a}\frac{\partial}{\partial\phi}\left(\frac{g}{af\cos\phi}\frac{\partial\ \Delta h}{\partial\lambda}\right.\right] &= \Delta\tilde{q}
\end{aligned}$$

where we have used the notation defined in section 2.2.3, page 28. This is a very complicated and expensive equation to solve for the correction, considering that we have chosen the coefficients using tunable parameters. We therefore wish to

simplify it to reduce the computational cost involv

equations 3.6 and 3.8

$$\Delta h = - \ \delta \ \ \Delta U + \delta_{\phi c}\Delta V \qquad 3.28$$

$$\Delta u_0 = -\overline{\left(\left(\overline{\frac{\Delta U}{\overline{h}}}^{\phi} \ \delta \ \ u_0\right)\right)} - \frac{\Delta V}{\overline{h}^{\phi}}\delta_{2\phi}u_0 + \overline{\left(\frac{\Delta U}{\overline{h}}v_0 \right.}^{\phi}\frac{tan\phi}{a} - g\delta \ \ \overline{\Delta h}^{\phi} + \frac{f\Delta V}{\overline{h}^{\phi}} \qquad 3.29$$

$$\Delta v_0 = -\frac{\Delta U}{\overline{h}}\delta_2 \ \ v_0 - \overline{\left(\left(\overline{\frac{\Delta V}{\overline{h}^{\phi}}} \ \ \delta_{\phi}v_0\right)\right)}^{\phi} - \frac{\Delta U}{\overline{h}}\overline{u_0} \ ^{\phi}\frac{tan\phi}{a} - g\delta_{\phi}\overline{\Delta h} \ - \frac{f\Delta U}{\overline{h}} \qquad 3.30$$

where Δ represents the difference between the true values at the new time level and the curren

If we were to continue following the procedure of section 3.1.2 we would now need to substitute for ΔV in equation 3.33 using equation 3.34 and for ΔU in equation 3.34 from equation 3.33 . However because of the averaging incurred by using the staggered grid this would cause the equations at any point to be coupled to the equations at all other points. The effect of the coupling decreases with distance from the point about which the original substitution is performed. However it is not practical to pursue this line and so we seek to simplify the equation accepting the penalty that we shall not be able to remove all the residual in one go. This is similar to omitting the term in the SIMPLEC algorithm which leads to a simpler scheme at the expense of extra iterations, see Van et al. [73] and Wen et al. [76]. We require that the iteration we construct must converge to the same solution as that obtained for the full equation, and this has yet to be proven. We can avoid the coupling if we neglect the terms involving ΔV in equation 3.33 and ΔU in equation 3.34 . If we also neglect the ϕ derivative of ΔD in equation 3.33 and the λ derivative of ΔD in equation 3.34 since these terms are order f smaller than the derivatives of ΔD in the other co-ordinate direction in the respective equations, then we obtain the reduced equations

$$g\delta\ \Delta D - f\left[f + \frac{1}{\overline{h}}\delta_2\ v_0 + \frac{1}{\overline{h}}\overline{u_0}^{\ \phi}\frac{tan\phi}{a}\right]\Delta U = R_{ew} \qquad 3.35$$

$$g\delta_\phi \Delta D - f\left[f - \frac{1}{\overline{h}^\phi}\delta_{2\phi}u_0\right]\Delta V = R_{ns} \qquad 3.36$$

For simplicity we define

$$A = \frac{1}{f\left[f + \frac{1}{\overline{h}^\lambda}\delta_2\ v_0 + \frac{1}{\overline{h}^\lambda}\overline{u_0}^{\ \phi}\frac{tan\phi}{a}\right]}$$

$$B = \frac{1}{f\left[f - \frac{1}{\overline{h}^\phi}\delta_{2\phi}u_0\right]}$$

Then taking the divergence of equations 3.35 and 3.36 we obtain away from the equator

$$\delta\ \ gA\delta\ \Delta D\ + \delta_{\phi c}\ gB\delta_\phi \Delta D\ - \Delta D = \delta\ \ AR_{ew}\ + \delta_{\phi c}\ BR_{ns} \qquad 3.37$$

which is elliptic if the data is inertially stable, and we have shown in section 3.2.3 that this is easily enforced. This ellipticity condition is much simpler than the one derived in section 3.1.2 and is a necessary but not sufficient condition for the full ellipticity condition to hold. We now need to derive the equation at the equator. In section 3.1.2 we noted that if we enforce inertial stability on the data then we have removed the residuals on the equator. When we enforce inertial stability we do so only on the balanced velocities and not on the height field. This is because of the difficulty in enforcing

$$f\left[f+\delta\ \left(\frac{g}{f}\delta\ h\right.\right.\ +\overline{\left.\left.\left(\frac{g}{f}\frac{tan\phi}{a}\delta_\phi h\right.\right.}^{\phi}\right]\geq 0$$

and

$$f\left[f+\delta_\phi\left(\frac{g}{f}\delta_\phi h\ \right.\right]\geq 0\,,$$

for which no effective numerical method could be found. Thus we are unable to continue to follow the approach of section 3.1.2. We note that an alternative to enforcing the Neumann boundary condition at the equator is to use a Dirichlet condition since all the results we have used for elliptic equations hold equally for this type of boundary condition. This leaves us with the problem of finding the solution at the equator before we can solve for the rest of the domain. The equation we need to satisfy at the equator is

$$\delta\ \Delta D = R_{e\,w} \tag{3.38}$$

since the other balance equation is formed half a grid-length polewards of the equator where $f \neq 0$. 3.38 is easily solved to give

$$\Delta D = e\ \lambda\ +s\ \phi$$

where $e\ \lambda$ is the solution of equation 3.38 and $s\ \phi$ is some arbitrary function.

Fourier coefficient a_0 in a Fourier expansion of the solution ΔD in the $\lambda-$direction giv

those made to derive the reduced equation 3.37 and at worst should just add extra iterations to the procedure. Using this method to find a_0 and then solving equation 3.37 with the Dirichlet boundary condition does produce a noticable unremoved residual at the equator in the multigrid solution on the first application of the corrector step on a timestep, which is removed on the subsequent iteration of the corrector step. No adverse effects appear from this unremoved residual and idealised experiments with the multigrid code suggest that the error may be entirely due to the multigrid algorithm, and not because of the simplifications made here, see section 3.3.4. The results gained via the solution of the reduced equation 3.37 and the Dirichlet boundary condition method are given in the next chapter, and as we saw in section 3.1.4 these simplifications do not appear to be detrimental to the solution in any way, except perhaps in a slight

the rotational part of the wind field is undefined at the equator. We choose to set the rotational part of U to zero at the equator, and since it is not used anywhere

3.2.5 The Complete Procedure

The full predictor/corrector scheme can be summarised as follows

Step 1 q dependent diffusion.

Step 2

3.3 ultigrid thods on th Sph r .

3.3.1 Introduction to Multigrid methods.

Many problems in computational mathematics require fast, accurate solutions to elliptic partial differential equations. If we consider the model problem,

$$\frac{\partial^2 Q}{\partial x^2} = f\ x$$

on a periodic domain, then if we discretise using, for example, centred finite-differences we obtain the matrix system,

$$A\underline{Q} = \underline{F}$$

where A is a square, symmetric tri-diagonal matrix. Fast direct methods exist for such a problem. If we now consider the more complicated equation,

$$a\ x,y\ \frac{\partial^2 Q}{\partial x^2} + b\ x,y\ \frac{\partial^2 Q}{\partial y^2} = f\ x,y$$

and again discretise we obtain a block tri-diagonal matrix system. For a $N \times N$ problem the cost of direct solution is $O\ N^6$ and takes $O\ N^4$ elements of memory

equations the *Multigrid* method has usually been shown to be the best iterative procedure, see Gary et al. [29] for example.

The basic strategy behind multigrid is to choose a computationally cheap solver for the matrix problem, referred to as the *smoother*, and combine it with a procedure which solves the problem on a sequence of computational grids. Given the matrix system $A\underline{x} = \underline{b}$ then a simple iterative solver is the *Jacobi* iteration where we separate A into three matrices, a diagonal, a strictly upper diagonal and a strictly lower diagonal, denoted D, U, L respectively and form the iteration,

$$D\underline{x}^{n+1} = -\ L + U\ \underline{x}^n + \underline{b}$$

Convergence for the Jacobi iteration is quite fast for a few iterations and then becomes very slow. The reason behind this is easily understood by looking at the Fourier modes of the error $\underline{e} = \underline{b} - A\underline{x}$. The Jacobi method converges quickly for the high frequency modes, often refered to as the'rough' modes, of the problem but very slowly for the low frequency modes, often refered to as the 'smooth' modes. If we were to coarsen the problem by solving it on a grid with half as many nodes then the Jacobi method would now converge quickly for the 'rough' modes on this new coarser grid. We need to be able to perform this coarsening without changing the solution to the problem. This suggests the following procedure, here shown for just 3 grids.

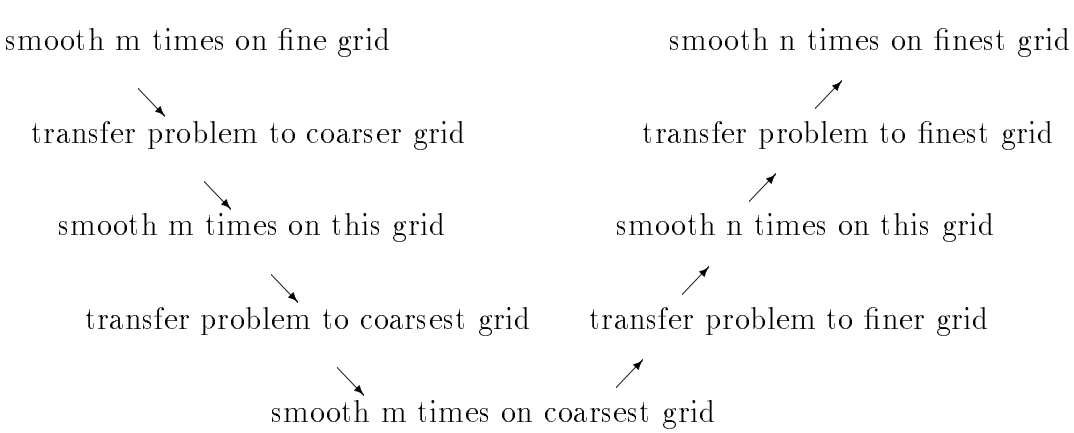

The method shown above is called a m,n V-cycle multigrid method. The V comes naturally from the shape and the m,n describes the number of smoothing

optimum scheme for an

We wish to solve the problem on an $M \times N$ equally spaced grid in λ, ϕ space where M is even and N is odd. We define $\Delta\lambda = 2\pi/M$ and $\Delta\phi = 2\pi/\ N-1$. We denote by $Q_{i,j}$ the value of Q at $\quad i-1\ \Delta\lambda, \pi/2 -$

grid in the results in table 3.1 in section 3.3.4. This may also not be desirable if, as is required here, line solvers must be used as the smoother. This is because the matrices generated by the line solvers becoming increasingly complicated and more expensive to solve.

3.3.3 Implementation

Definition of convergence.

We need to define when convergence has occured. There are two commonly used definitions which measure the performance of the multigrid scheme. We define the root mean square residual for the matrix problem $Ax = b$ as

$$rms = \left[\frac{1}{s} \sum_{i=1}^{s} b_i - Ax_i \ ^2 \right]^{\frac{1}{2}}$$

where s is the number of elements of x. The first measure of convergence is the *Multigrid Convergence Rate* henceforth MCR which is defined simply as the root mean square residual at the end of a V-cycle divided by its value at the start of the V-cycle. The second measure is called *the Practical moothing Rate* henceforth PSR and is defined for a m,n V-cycle as,

$$MCR^{\frac{1}{m+}}$$

examples considered later we generally get a PSR value between .35 to .40 for all V-cycles except the last one or two. A good cutoff value for defining convergence has proved to be .950. This is because the scheme can often perform many more V-cycles with values around .97 to .99 before reaching a value of 1 but they gain us little extra benefit for often a substantial cost.

We note that it is not uncommon for certain problems for some iterative procedures to reach a plateau after a certain number of iterations. The scheme may remain there for many more iterations before once more converging quickly. This

beha35obhcatl97yget–maute–n–ce4–ee““TD4–eren–t““TD4–kTj4“–Thepublister–msults–i–tTJ4ugge

This was discussed in section 3.2.1, page 66. We note that as we change grids the value at the poles will change whilst the other values remain the same. However the polar cosine value can always be obtained simply as $\Delta\phi/4$ on any grid.

Grid sequence.

The grid sequence generated depends on whether we are solving the global or hemispheric problem.

In the λ-direction we require all grids to have an even number of points since this allows us to apply restriction by simply taking alternate grid points. This constraint could be removed but would require a more complicated restriction and hence is probably undesirable. Secondly the minimum number of points allowed

e teeconoodeor

Grid Index	λ	ϕ
6	192	129
5	96	65
4	48	33
3	24	17
2	12	9
1	6	5

Thus we end up with a 6×5 problem to solve on the coarsest grid, the grid generation being stopped by the ϕ

next grid down. The reason behind numbering the coarsest grid 1 is that if we add more points then it is easier to see the structure growing.

Smoother.

We consider the problem $Ax = b$. We wish to smooth the rough modes of the error so we calculate the residual,

$$r = b - Ax_1$$

where x_1 denotes the current solution and solve the correction equation for Δx,

$$A\Delta x = r$$

and then update the solution by

$$x_2 = x_1 + \Delta x$$

The question is thus which is the optimum iterative solver for the correction equation ? The solver must smooth the rough modes on all grids and be as computationally inexpensive as possible. The problem on the sphere is that we are not dealing with a square grid in cartesian space but with one with strong anisotropies. Consider again our example grid of 192×129 and calculate the ratio of $a\Delta\lambda cos\phi$ to $a\Delta\phi$.
on Row 2 we get, 30.5 : 1
on Row 33 we get, 1 : 1
on Row 65 we get, 0.75 : 1
From this it is obvious that towards the poles the problem is more strongly coupled in the λ-direction than in the ϕ-direction and to a lesser extent the converse is true as we approach the equator. For problems exhibiting these strong anisotropies the usual point smoothers used in many multigrid algorithms have very poor

smoothing properties. However, line smoothers do smooth v

terms of the number of V-cycles required. However the Zebra line relaxation offers the benefit of being vectorisable on a CRAY Y-MP computer and thus is significantly cheaper on this particular architecture, by a factor of between 6 and 8 times. The Zebra scheme is also well suited to parallel computer architectures, although wb et to implementthe scheme on a massively parallel computer. We consider to implement multigrid on a m

section 3.3.5. The poles are treated as follows. No λ-direction l

poles. In the λ-direction line solver, each line is solved for all th

Restriction.

We choose to perform the restriction by taking alternate points in each direction and we have to restrict the fields, A, B, C, Q, R and the trigonometric functions. Since the coefficients and the trigonometric functions are the same for every V-cycle w

by r, given by

$$r$$

point i, j not at the pole is

$$\frac{1}{16cos\phi_i}\begin{bmatrix} rcos\phi_{\ i-1,j-1} & +2\ rcos\phi_{\ i,j-1} & +\ rcos\phi_{\ i+1,j-1} \\ +2\ rcos\phi_{\ i-1,j} & +4\ rcos\phi_{\ i,j} & +2\ rcos\phi_{\ i+1,j} \\ +\ rcos\phi_{\ i-1,j+1} & +2\ rcos\phi_{\ i,j+1} & +\ rcos\phi_{\ i+1,j+1} \end{bmatrix}$$

This is simply a grid box area weighted version of the 1-D full-weighting applied in 2-D. To complete the restriction we need the equivalent definition at the pole. The condition we must satisfy is, if

$$\sum_{fine} r\Delta\lambda cos\phi\Delta\phi = 0$$

then

$$\sum_{coarse} r\Delta\lambda cos\phi\Delta\phi = 0$$

where we sum over all points including every one at each pole. This is because of the way we chose to store the residual there. It is important to note, as pointed out in the section on data representation, that the polar cosine value changes as we change grids. Full-weighting at the pole, in this example the north pole, gives

$$\frac{r_{i,1}}{4} + \frac{1}{8cos\phi}$$

rep

Prolongation.

The only field we need to transfer to a finer grid is the current value of the answer Q. This is done by linear interpolation since this it is cheap and also the inverse of the full-weighting restriction operator up to an arbitrary constant. The combination of linear interpolation and full-weighting restriction is probably the most commonly used in multigrid schemes. It is also probably the easiest to use in the standard multigrid smoothing analysis.

3.3.4 Results.

For the momenQ

difference equation for the λ-direction line solver is

$$\frac{1}{a^2 cos^2 \phi_{i,j} \Delta\lambda^2}$$

Dimensions	Grids	Init. Res.	Final Res.	V-cycles	CPU	Scaled CPU
24 x 17	3	$.186\text{x}10^{1}$	$.309\text{x}10^{-9}$	7	0.069	$2.42\text{x}10^{-5}$
48 x 33	4	$.247\text{x}10^{1}$	$.173\text{x}10^{-9}$	8	0.179	$1.41\text{x}10^{-5}$
96 x 65	5	$.278\text{x}10^{1}$	$.902\text{x}10^{-10}$			

smallest problem which takes one fewer cycle. Allowing as many grids as possible is obviously beneficial from the example of the 384×257 problem where when we allow one less grid, although the solution still converges to the same accuracy, it takes 5 more cycles. Finally we look at the cost. The cost of multigrid methods usually scales order $n \, log \, n$ where n is the number of points but we see from the scaled CPU that the cost scales better than order n. This is because the CRAY

global problem and the results are given in table 3.2.

We note that once again we verify the grid independence assertion for this exam-

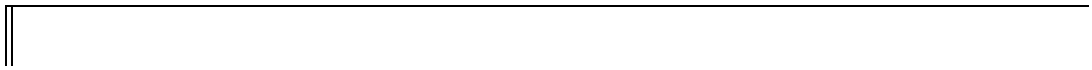

grid is determined by the boundary condition, the boundary condition must be transferred so as to be consistent with the transferred problem on that grid. The worsening results for the hemispheric problem suggest that more grid transfers equals a poorer solution and that we have not achieved this consistency. For this relatively easy problem it is probably possible to construct a restriction operator which will alleviate this fault. However for the more general problems that we wish to solve, for example equation 3.37 this is not possible and the presence of this error is of some concern.

$$B = \frac{1}{sin^2\phi}$$

$$C = 1$$

$$\begin{aligned} RHS &= -sin^2\phi cos^2\phi sin\lambda + 1. - 2sin\lambda - 2sin^2\lambda \\ &\quad + sin\lambda\ 4 - \end{aligned}$$

throughout, provided that this is not zero except possibly at the equator. However, for general coefficients, there is the problem that they are inside a partial derivative and care must be exercised in this re-scaling to avoid leaving divisions by zero in the code. In practice the coefficients need to be differentiated out to leave a system which includes terms involving both first and second derivatives of the solution and first derivatives of the coefficients. To apply centred differences to this system requires averaging of derivatives and coefficients in parts of the discretisation which can lead to a loss of accuracy.

We now return to the question of whether the 2,3,2 V-cycle is optimum and also whether or not we require alternating line relaxation. To investigate these questions we consider again Poisson's equation on the sphere using the hemispheric version of multigrid at 384×257 resolution. Due to changes in the maths library routines used to calculate trigonometric functions on the Cray Y-MP the result for the 2,3,2 V-cycle with alternating line relaxation is not identical to the one obtained earlier. All comparison results quoted here and elsewhere were performed consistently, in the sense that any results compared used the same maths library routines. For the results in table 3.4 all the schemes converged to the same degree of accuracyeraging line A eragi“q4“““““cm4Im“Do4QBT4wit“q4“““TD4““cm4I

From table 3.4 it is easy to see that for this problem there is no need for the alternating line scheme as the λ-direction line solver on its own converges to the same accuracy in the same number of cycles. Using the λ-direction only solver reduces the cost by over 50% in this example. To test if this held true for solving the correction equation 3.37 from the previous chapter idealised data runs were performed with the alternating line and λ-direction only schemes using the 2,3,3 V-cycle. The following times were obtained for the first order in time semi-Lagrangian solution of thethl""TD4"Ts data

to just one on the descending branch. This scheme produces a further saving and for this problem the 1,3,2 V-cycle λ-direction only scheme has been found to be optimal on one processor of a CRAY Y-MP. Using the 1,3,2 V-cycle λ-direction only scheme for the idealised McDonald-Bates problem gives a CPU time of 925 seconds which is a modest saving compared to that gained by not using the alternating line scheme. Again no significant impact on the solution was noticed with this version of multigrid and we can use any of the multigrid schemes to obtain the solution if we are not concerned about the amount of CPU time used.

3.3.5 Discussion of future developments and parallelisation aspects.

We intend to extend the code to 3-dimensions but before proceeding too far in this direction it is necessary to consider performance aspects closely. For the moment we shall be running the code on a CRAY Y-MP 8-64 computer which has 8 processors and 64 megawords of memory. The 2-D code used only 1 processor and only just over 3 megawords of memory for the largest problem we considered in the previous section. We shall ignore memory considerations as these are not of primary concern. The question is how to make most use of the computer architecture to obtain the best execution time. The CRAY uses a shared memory architecture and when using microtasking it behaves as an SM-SIMD machine. Shared Memory Single Instruction Multiple Data, hence SM-SIMD, is based on the principle that all memory is central and shared, with the same piece of work being allocated to each processor but working on a differe“TD4 oc–primary

Regardless of the smoother we use as we coarsen the grids we leave fewer and fewer points at each node and performance deteriorates. One way to get around this is to limit the minimum number of points each processor can have, however this restricts the number of grids we can generate and we have already seen how this can significantly increase the number of iterations required. To make things even worse as we add more processors to increase our computing power the performance of multigrid can get worse. One solution is to use a system called *agglomeration* where we keep the granularity high by coarsening and keeping the numbers of points on some processors large at the expense of leaving some with no points at all. Thus we are effectively reducing the number of processors working. This has the disadvantage, in practice, of increasing the length of the communication links but can gain some extra efficiency and does not increase the number of iterations required. Smith and Fiddes [71] noted that implementing multigrid without aglomeration was significantly more complicated than other iterative solvers, for example conjugate gradient, on a DM-MIMD machine. Other authors, for example Linden et al. [40] and Robinson [62], have successfully implemented multigrid on parallel architectures with varying degrees of success and much work will no doubt continue in this area. However, of more concern is that no one has considered, as far as we know, the problem of including line solvers rather than simple point solvers. Naik and V

case semi-coarsening degenerates to the so-called *algebraic* multigrid method. In this method we generate all possible grids by restricting all current ones in one direction at a time. We then solve on each. This requires a more complicated set of restriction and prolongation operators as we need ways to combine answers from various grids. A simple 8×8 example of all the grids generated, assuming a minimum number of 2 points in each direction, exhibits all the salient features;

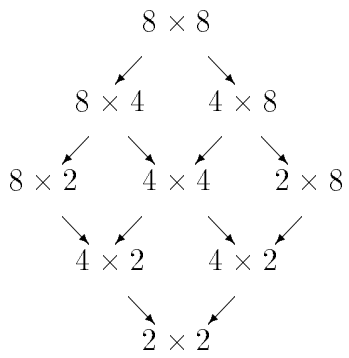

We note for example that to obtain the problem on the 4×4 grid we need to combine the information from the 2 grids above it. This combination is not necessarily a simple addition but depends again on anisotropy and the problem. However, it may prove to be worth the effort on a DM-MIMD machine where line solv

Chapter 4

Computational Results

In this chapter we present computational results for several idealised and real data cases using the predictor/corrector method described in the last chapter. We compare the performance of the various advection schemes on one of the idealised problems, and also on real data. We also compare results with those obtained from a C-grid primitive equation model, the semi-Lagrangian model of Bates et al. [7], henceforth PE. Before we do this we need to explain how initial

and hence $\partial \underline{u_0}/\partial t$ by solving the elliptic equation for $\partial h/\partial t$. However the initial height field may not satisfy these constraints, as typically happens when using 500 hpa height fields from operational forecast models. Also many idealised problems used to test the shallow-water equations suffer from the same failing, for example the problem of McDonald and Bates described in section 4.2.1 is inertially unstable near the equator, and the Rossby-Haurwitz wave problem, section 4.2.2, has areas of negative q. We cannot use the direct method to find the other fields when we do not have an initial height field which satisfies the constraints, and so we have developed the following initialisation procedure for the SSG model.

Initialisation stage 1.

We take the initial height field and iterate the correction step from the predictor/corrector method but updating only the balanced velocity field $\underline{u_0}$. We perform k iterations of this procedure which gradually fits $\underline{u_0}$ to the height field where possible. In areas where the height field violates the conditions required to find the other fields directly, the inertial stability constraint applied to the $\underline{u_0}$ field prevents the balanced wind field from satisfying the balance equations for this illegal height field. The procedure can be sumarised as

iterate k times

Step 1 Corrector step. Updating $\underline{u_0}$ only.

Step 2 Inertial stability enforced.

Initialisation stage 2.

The second stage of the procedure is to take the fields at the end of the first stage and apply the correction step procedure again but now allowing h to be updated

as well. In areas where a v

the initial data.

For all the problems we consider in this section typical numbers used in the initialisation procedure are, 60 iterations of the first stage of the initialisation procedure and 30 iterations of the second stage. The most important thing to achieve is to fit the balanced wind field to the height wherever possisei

tial data using the predictor/corrector method of the previous chapter with three different prediction schemes. The first is the semi-Lagrangian scheme with first order accurate trajectories; w

fields, figure 4.9 for the semi-Lagrangian scheme and figure 4.11 for the Fourier damped Heun, look very similar. Comparing them with those obtained for the 1800 second timestep run we notice a further increase in the height at the centre of the high to 6534 metres, the low is also more intense. Looking at the q fields, figures 4.10 and 4.12, we notice that away from the pole they again agree very well, but whilst the semi-Lagrangian solution still has a smooth circular 40 unit contour the Fourier damped Heun scheme has started to fragment this feature.

To further compare the various schemes we investigate the accuracy of the schemes for real data. Here we use the real data simply to look at accuracy and leave the discussion of the results until section 4.3. 2 day integrations from the initial data of 1st February 1991 were performed, running with a 1800 second timestep and we take as the true solution a semi-Lagrangian run with a 300 second timestep and second order accurate trajectories. We evaluate the mean and max height differences between the three schemes we have looked at so far, plus the semi-Lagrangian scheme with second order accurate trajectories, and the calculated truth at the end of the 2 day integration. The results are in table 4.2.

Scheme	Mean Height Error m	Max Height Error m
S-L 1st	2.014	31.205
S-L 2nd	1.952	31.670
Heun FD	2.647	35.252
Heun LT	2.800	38.371

Table 4.2: Comparison of advection scheme errors.

We see that the semi-Lagrangian schemes have a considerably lower error than the Eulerian ones, although because the numbers are relatively small it is hard

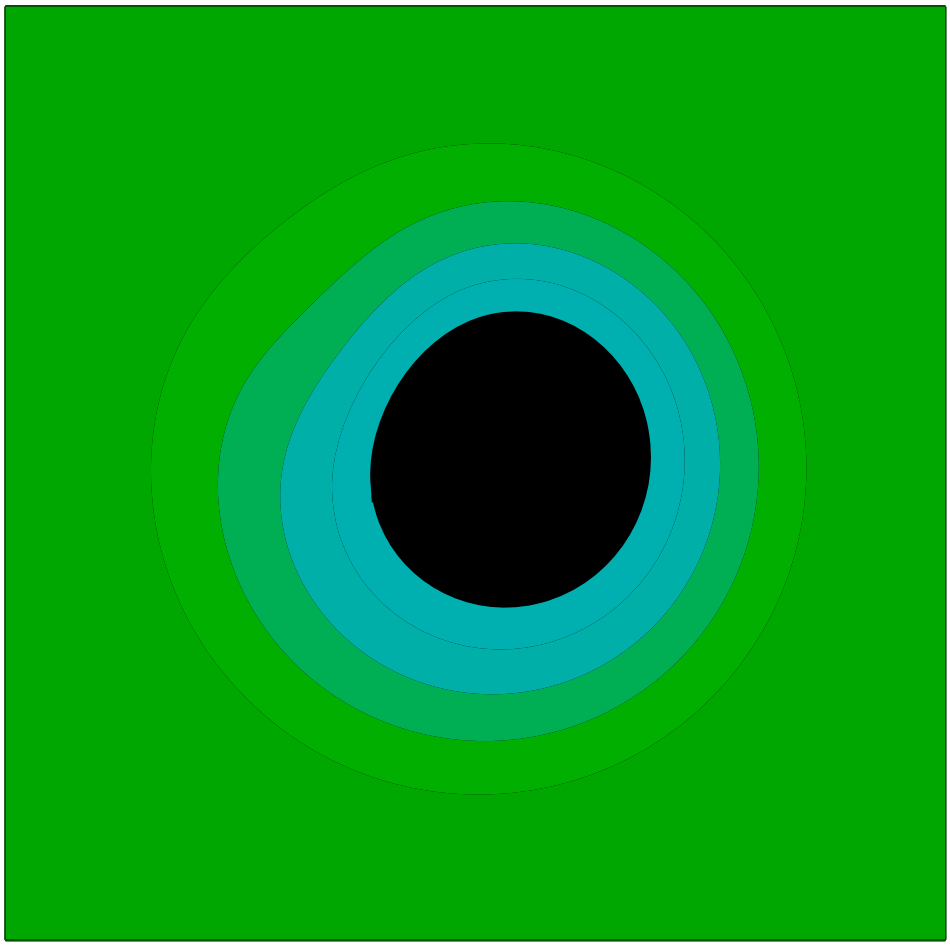

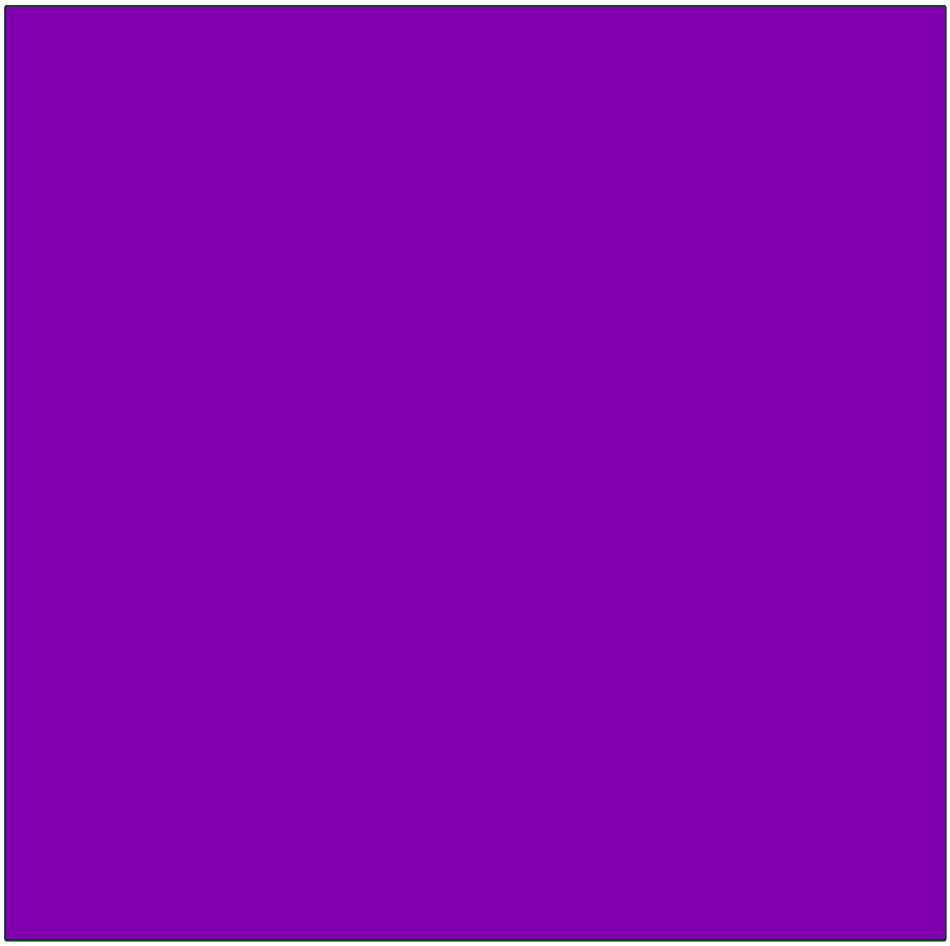

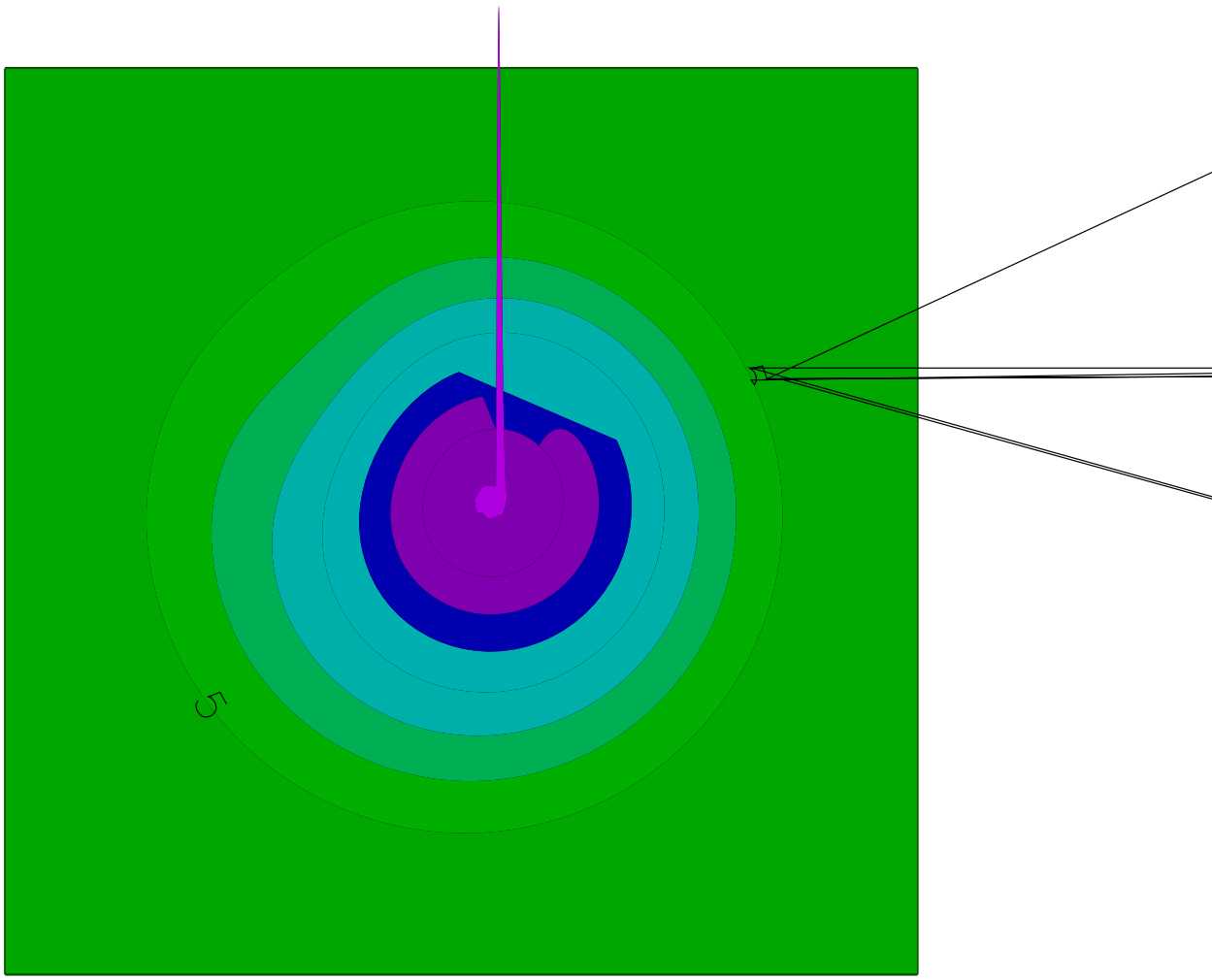
5

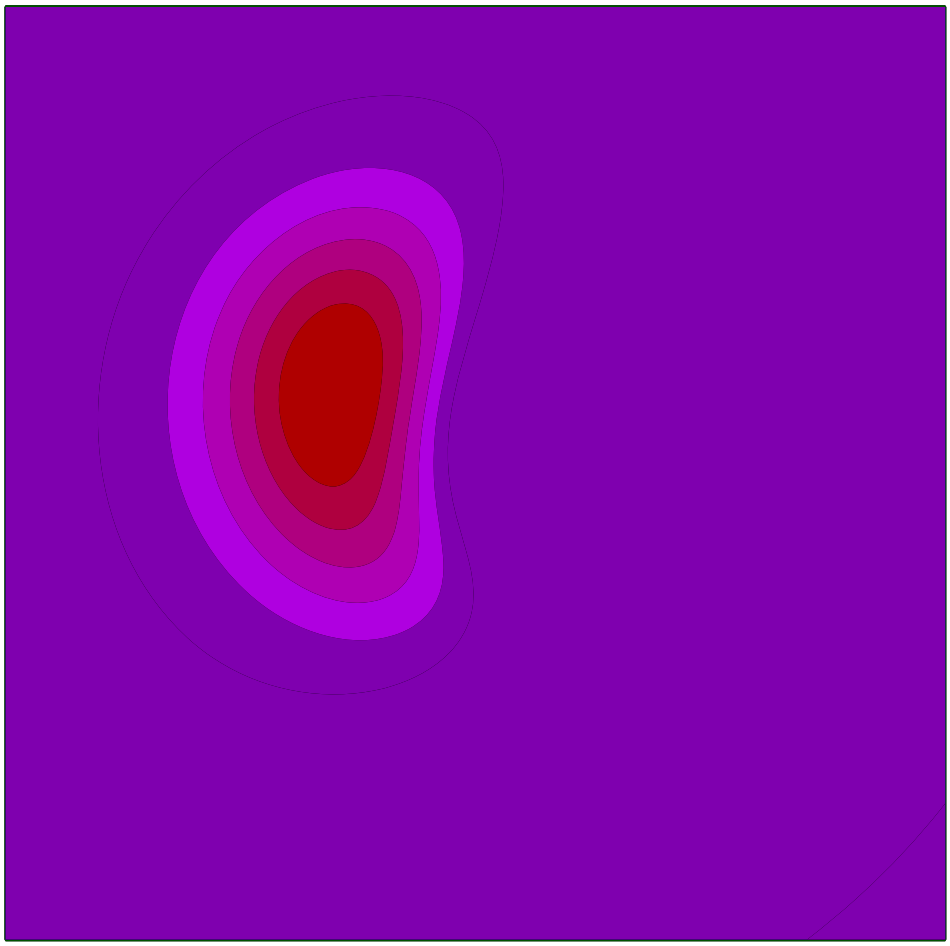

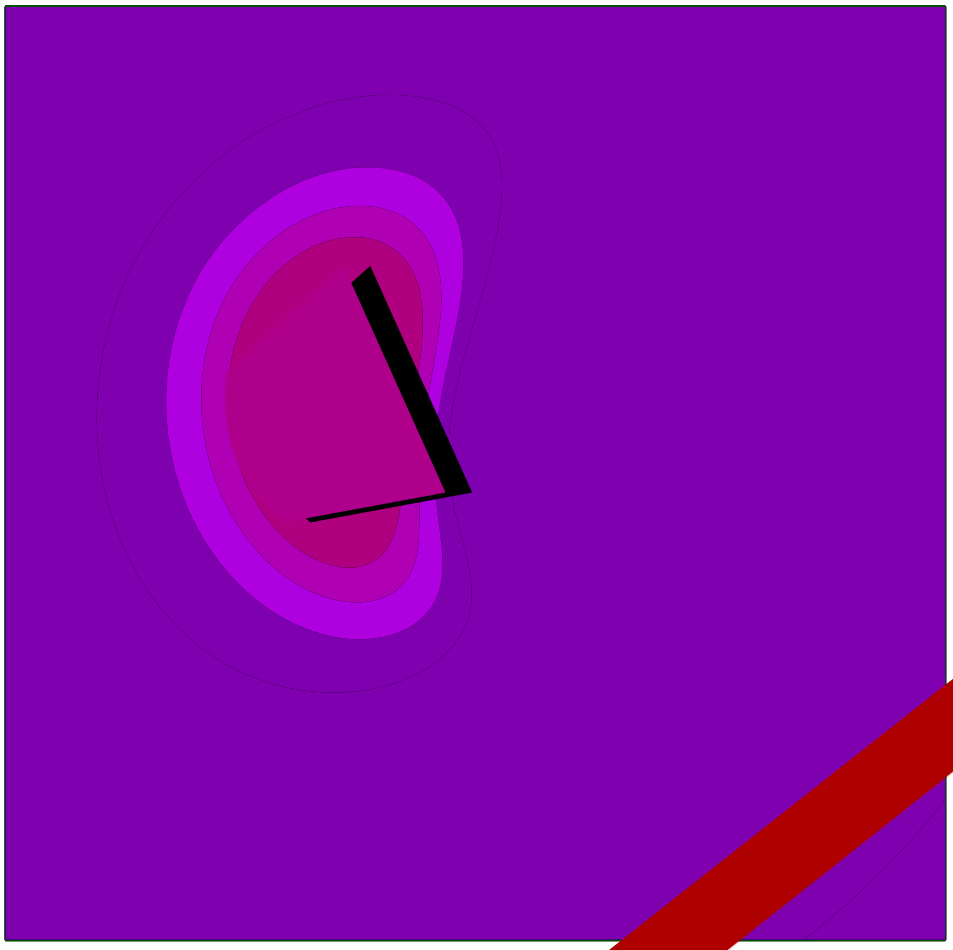

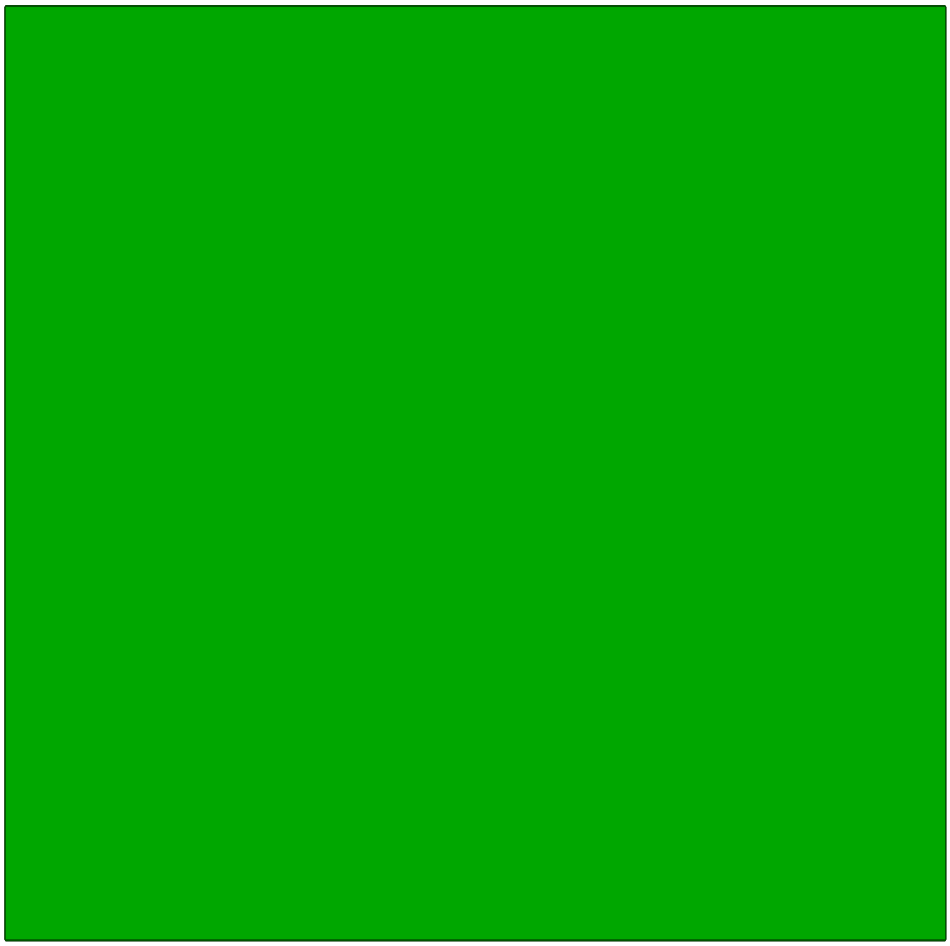

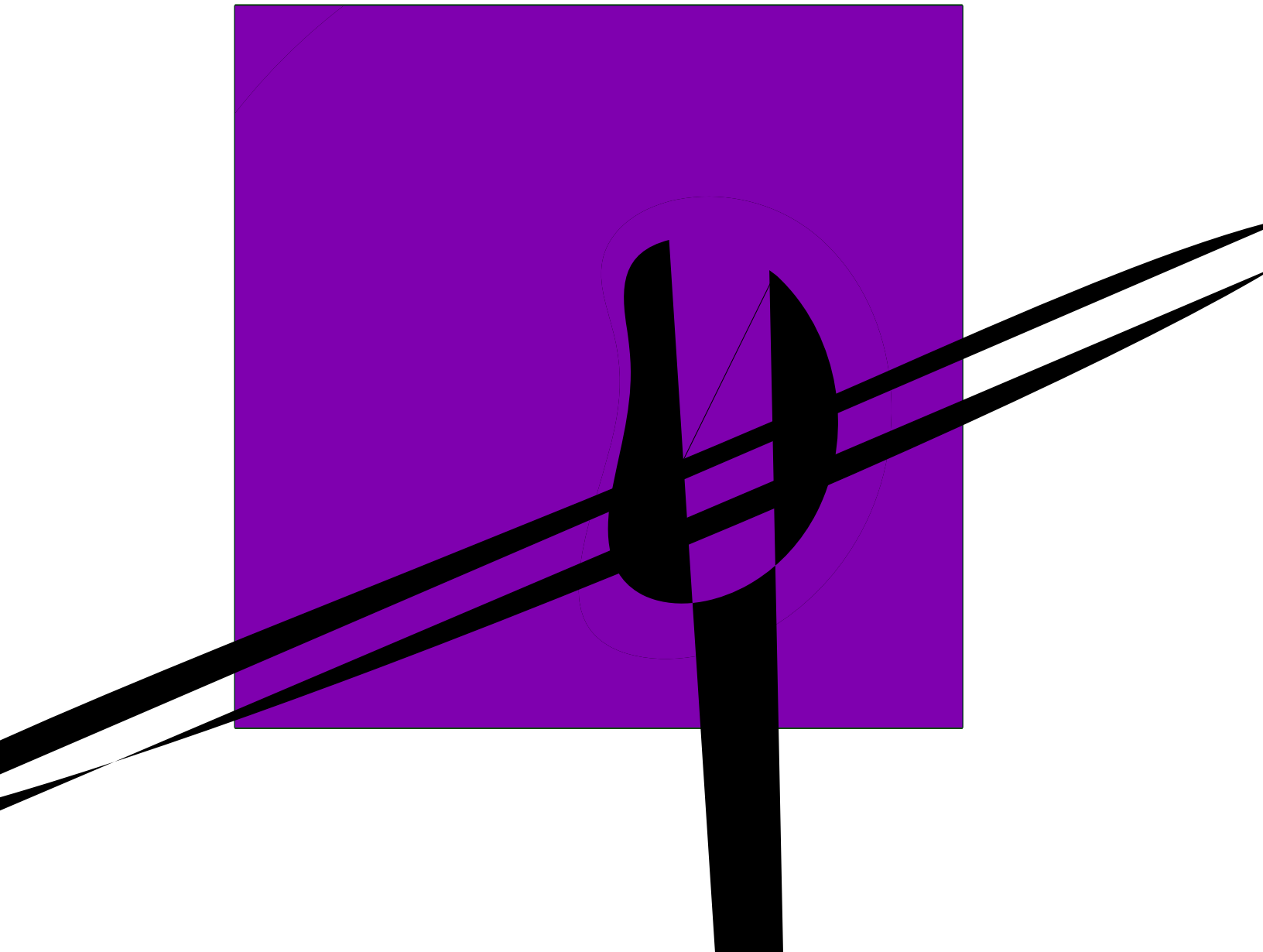

to see the differences when looking at charts of h, except in very small areas. The difference between the two semi-Lagrangian schemes is less significant, but the second-order accurate trajectories do yield a benefit for this timestep which agrees with the findings of McDonald and Bates [43]. We choose to use the semi-Lagrangian method from now on since we have seen that it is better able to represent features in the q field near the poles and has smaller errors. This has an added advantage in that when we compare with the primitive equation solutions we shall be using the same integration method in both models.

We now consider how the McDonald-Bates solutions from the SSG model compare with those from a primitive equation model. The PE model we use is the C-grid shallow-water semi-Lagrangian model of Bates et al. [7] upon which the semi-Lagrangian SSG model was based. The only major difference in the implementation of the semi-Lagrangian scheme in the PE model is that we use the semi-Lagrangian form of the mass equation, and not the Eulerian form used in the SSG model. This means that the PE model does not explicitly conserve mass, although deviations from the initial global mean value are very small. Figure 4.13 shows the height field after 5 days from the PE model with an 1800 second timestep. The initial field is almost exactly the same as for the SSG model, figure 4.1, and so we compare the solution with the initial data from the SSG model. We note that both high and low have lost intensity almost equally, approximately 110 metres. These solutions verify well with those found in Bates et al. [7]. Comparing the PE solution with the corresponding SSG semi-Lagrangian solution, figure 4.3, we see that unlike the PE model the high in the SSG model has grown slightly whilst the low has lost almost exactly the same intensity, 118 metres. The positions of the centres of the high and low agree quite well with the high very close to the same location, whilst the low in the SSG model is approximately 7 degrees east of the PE centre. Since the solution is rotating clockwise this implies

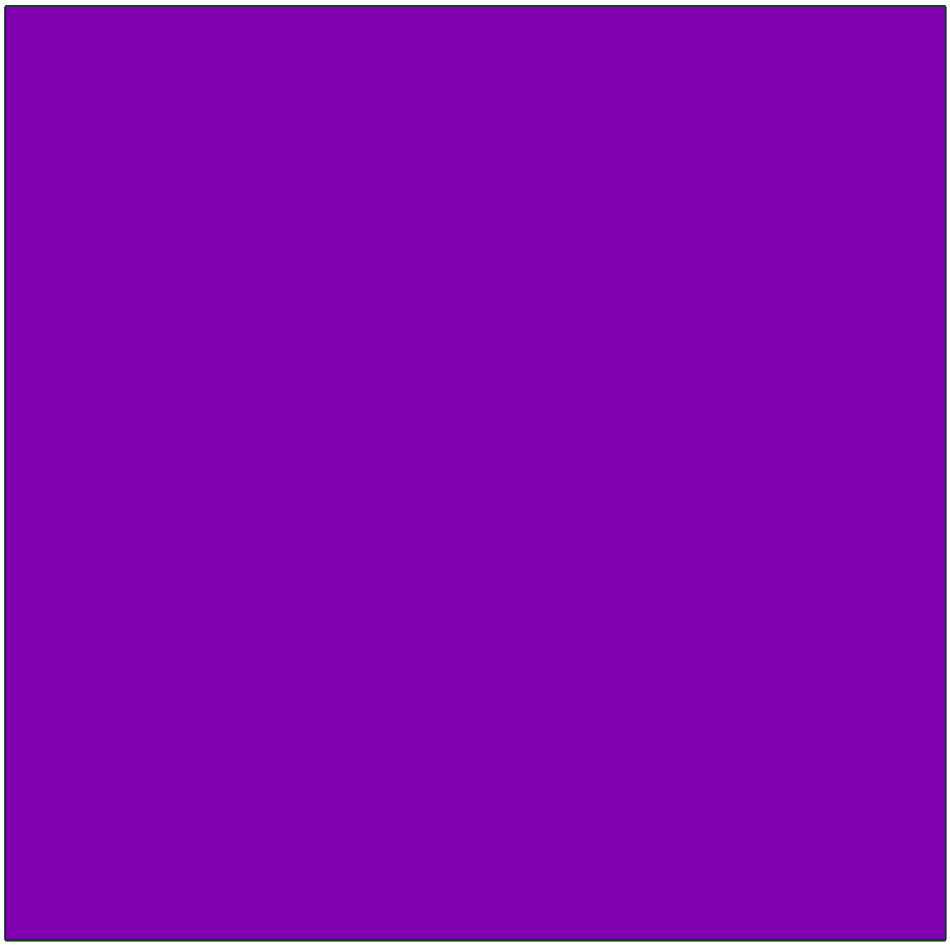

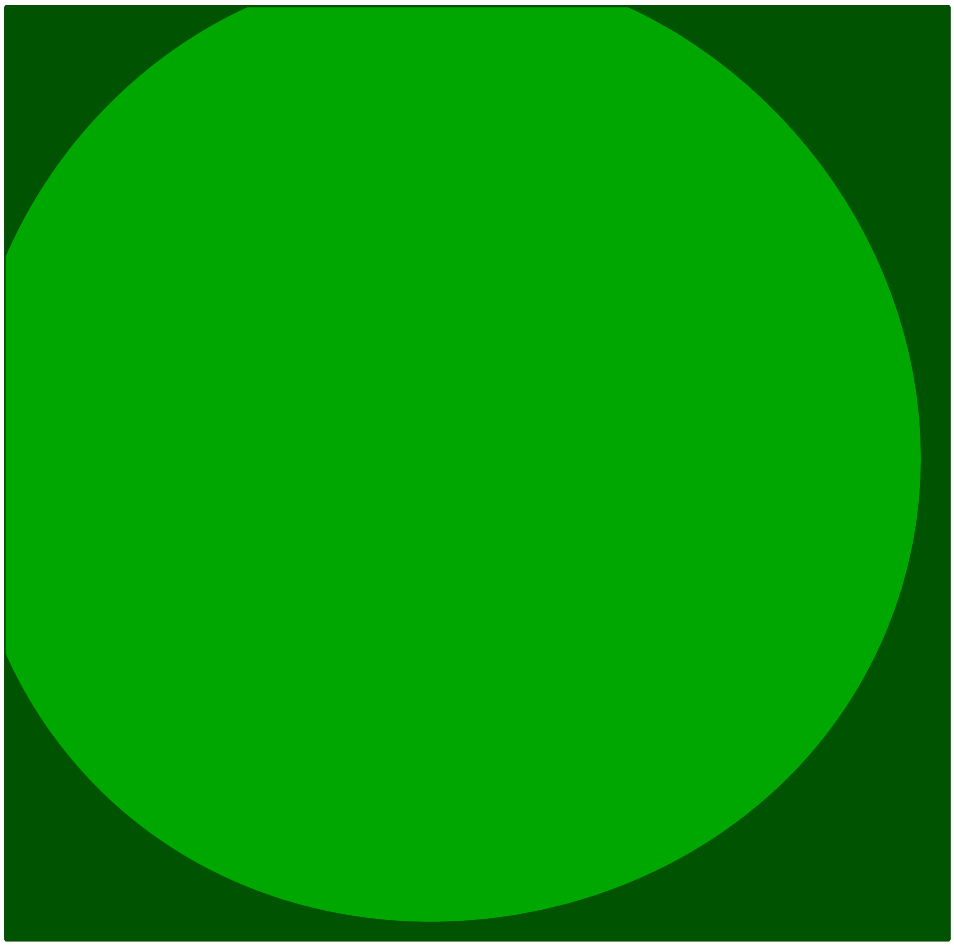

can be found in Phillips [57].

equations are,

$$\frac{\partial u_0}{\partial t} - 2\Omega v sin\phi = \frac{-1}{acos\phi}\frac{\partial \Phi}{\partial \lambda} \tag{4.1}$$

$$\frac{\partial v_0}{\partial t} + 2\Omega u sin\phi = \frac{-1}{a}\frac{\partial \Phi}{\partial \phi}\phi \tag{4.2}$$

$$\frac{1}{cos\phi}\left[\frac{\partial u}{\partial \lambda} + \frac{\partial v cos\phi}{\partial \phi}\right] = 0 \tag{4.3}$$

$$u_0 sin\phi = \qquad 4$$

equations have propagation speeds which are in excess of those for the SSG and primitive equations, as sho

no basic state zonal flow. For the parameters chosen for the numerical experiment the wave in the SSG model would have propagated 62 degrees in a non-divergent atmosphere, and this is in very good agreement with the 60 degrees that it propagated in the numerical experiment.

At this point we make some observations about the Rossby-Haurwitz wave as a simple representation of atmospheric motion. The atmosphere does not support the large amplitude oscillations at the equator required by the Rossby-Haurwitz wave and the propagation speed of the wave is much greater than that observed in the real atmosphere. The wave that can be represented by the SSG model is more typical of that seen in the real atmosphere, and the reduced propogation speed of the wave compared with the Rossby-Haurwitz wave is also much closer to

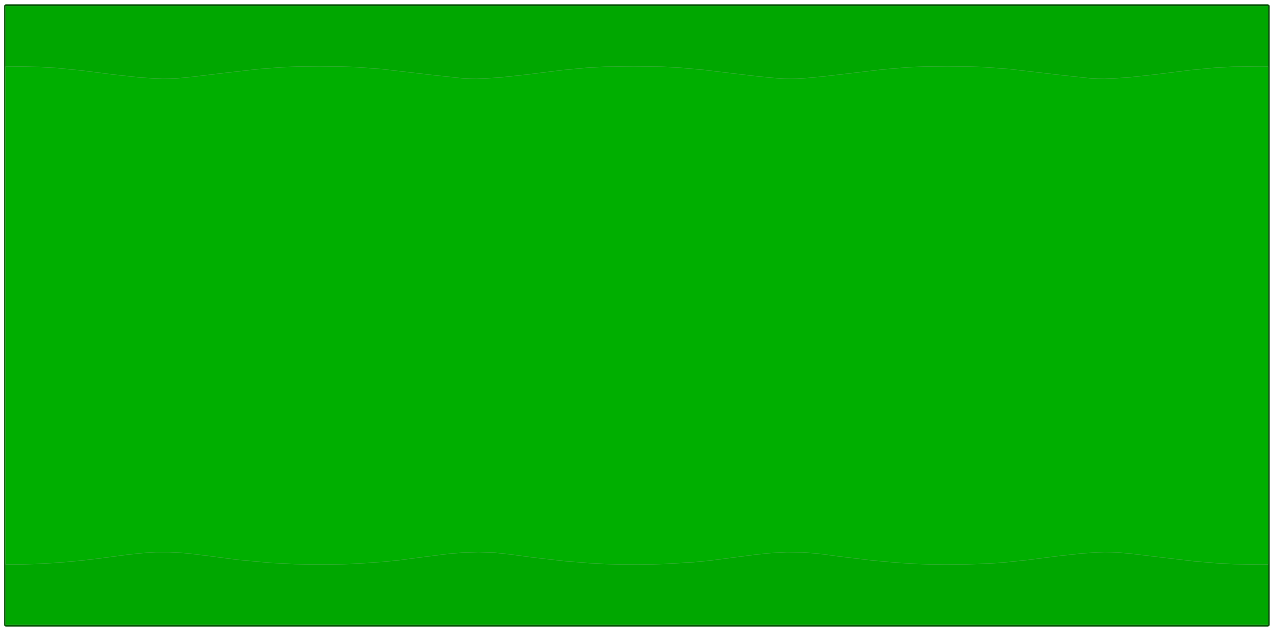

perform the same integration for the primitive equations. We take as our initial

phase speed for linearised non-divergent waves that are solutions of both equation sets. This suggests that the waves common in 500hpa flows are not of Rossby-Haurwitz type, and further enforces the view that the Rossby-Haurwitz wave is a poor representation of reality. The major areas of difference are in low latitudes where both models have formed high cen

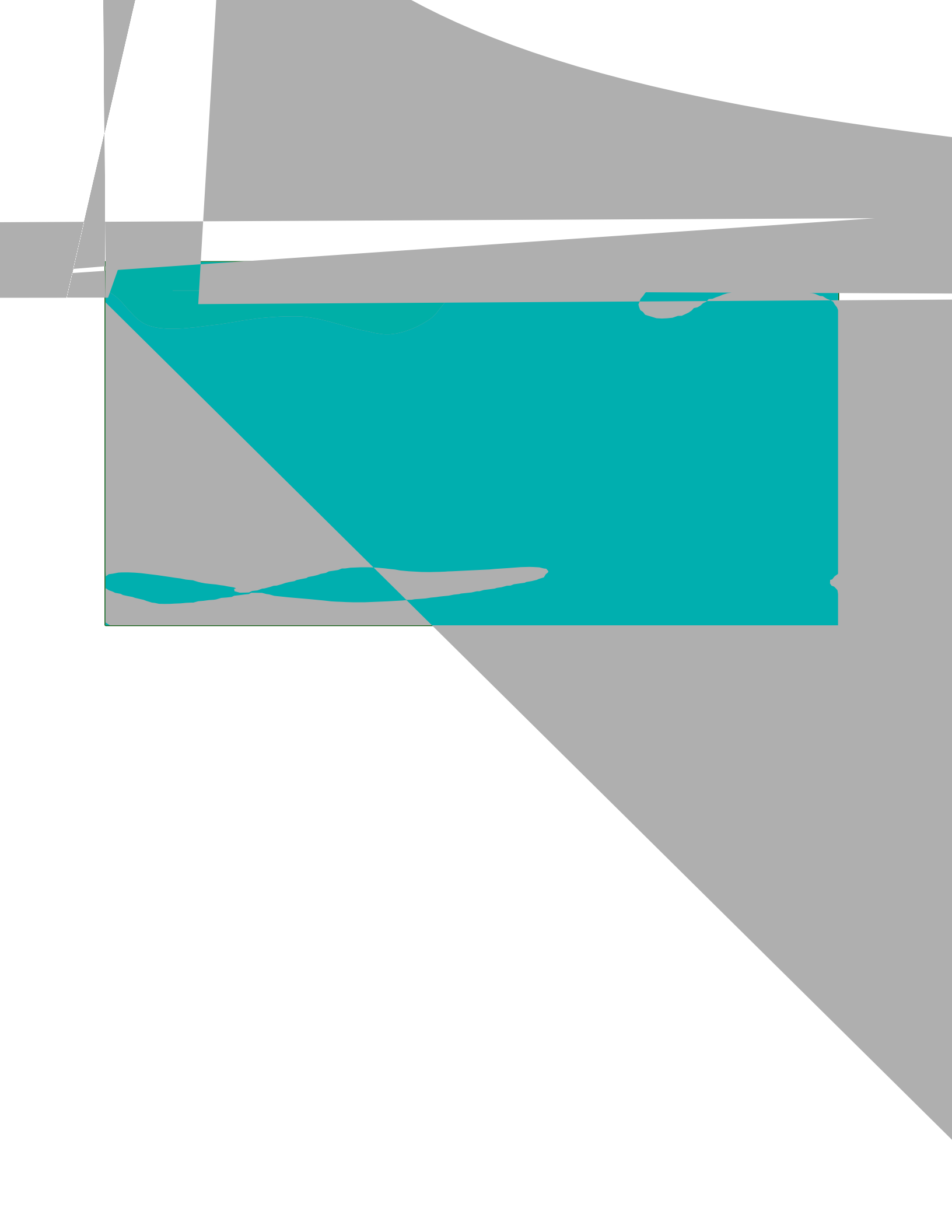

Chapter

Conclusions and Discussion

We begin by drawing conclusions from the work in this thesis before embarking on a brief discussion of the extension of the work to three-dimensions on the sphere and making a few comments on the inclusion of friction in the equations.

5.1 Conclusions

- We have been unable to prove the existence of a unique solution to the SSG equations on the sphere given certain constraints. However we have shown how this might be proven given that certain key propositions, 2.2 and 2.5, can be proven.

- A predictor/corrector method has been developed which is robust and appears, in numerical experiments at fixed spatial resolution, to converge to the analytic solution. A necessary part of the procedure has been the construction of a method which restores any solution which leaves the solution set of the equations back into it. This part of the numerical procedure is one area where more work may be required to find the optimum scheme.

5.2 Discussion

5.2.1 Extension to 3 dimensions

Following Hoskins [36] the 3-dimensional SSG equations may be written in spherical polar co-ordinates λ, ϕ, z as

$$\frac{D\underline{u_0}}{Dt} = S_p - \nabla_2\phi - 2\Omega\underline{k} \times \underline{u} \tag{5.1}$$

$$\frac{D\theta}{Dt} = 0 \tag{5.2}$$

$$\frac{1}{acos\phi}\frac{\partial u}{\partial\lambda} + \frac{1}{acos\phi}\frac{\partial\ vcos\phi}{\partial\phi} + \frac{\partial w}{\partial z} = 0 \tag{5.3}$$

$$\frac{g\theta}{\theta_{ref}} = \frac{\partial\phi}{\partial z} \tag{5.4}$$

$$\frac{g}{acos\phi}\frac{\partial\phi}{\partial\lambda} = fv_0 \tag{5.5}$$

$$\frac{g}{a}\frac{\partial h}{\partial\phi} = -fu_0 \tag{5.6}$$

where $\underline{u_0} = \ u_0, v_0\ $, $\underline{u} = \ u, v, w\ $, θ_{ref} is a reference θ value,

$$S_p = \left(\frac{uv_0tan\phi}{a}, \frac{-uu_0tan\phi}{a}\right.$$

$$\nabla_2 = \left(\frac{1}{acos\phi}\frac{\partial}{\partial\lambda} + \frac{1}{a}\frac{\partial}{\partial\phi}\right.$$

and

$$\frac{D}{Dt} = \frac{\partial}{\partial t} + u\frac{1}{acos\phi}\frac{\partial}{\partial\lambda} + v\frac{1}{a}\frac{\partial}{\partial\phi} + w\frac{\partial}{\partial z}$$

A similar approach to that in chapter 2 can be used to reduce this set of equations to one equation for $\partial\phi/\partial t$. Equations 5.1 and 5.2 can be used to obtain expressions for u, v and w in terms of u_0, v_0, θ and ϕ. Equations 5.4 - 5.6 can now be used to substitute for u_0, v_0 and θ in terms of ϕ and the resulting expressions for $\underline{u}$ in terms of ϕ can be substituted into equation 5.3 to obtain a single equation for $\partial\phi/\partial t$. We can follow the same approach as used in chapter

2 to try to prove the existence of unique solutions to this equation under the generalised versions of the conditions required in the 2-d case. It is anticipated that this extension will not prove difficult if the results required to show existence and uniqueness for the shallow-water problem can be proven.

The numerical procedure can also be extended to 3-d. We have one more predictive equation for θ and a 3-d version of the correction equations. The main problem in extending the numerical scheme lies in the extension of the method to restore solutions outside the solution set back into it. It may be that application of the 2-d procedure on each model level in the vertical along with insisting that $\partial\theta/\partial z > 0$, the static stability condition, will suffice. However, this an area where some work may be required.

5.2.2 Inclusion of friction

Cullen [16] discussed the inclusion of friction into this equation set, and in shallow-water form the equations become

$$\frac{D\underline{u_0}}{Dt} = S_p - g\nabla h - 2\Omega\underline{k} \times \underline{u} - C_D\underline{u_0} \tag{5.7}$$

$$\frac{\partial h}{\partial t} + \nabla .\ h\underline{u} \ = 0 \tag{5.8}$$

$$g\frac{1}{a cos\phi}\frac{\partial h}{\partial \lambda} = fv_0 - C_D u \tag{5.9}$$

$$g\frac{1}{a}\frac{\partial h}{\partial \phi} = -fu_0 - C_D v \tag{5.10}$$

where

$$S_p = \left(\frac{uv_0 tan\phi}{a}, \frac{-uu_0 tan\phi}{a} \right.$$

and the Eulerian form of the derivative is

$$\frac{D}{Dt} = \frac{\partial}{\partial t} + u\frac{1}{a cos\phi}\frac{\partial}{\partial \lambda} + v\frac{1}{a}\frac{\partial}{\partial \phi}$$

with C_D the drag coefficient. More complex functions representing frictional effects can readily be included. Assuming that the drag coefficient is constant then it can be shown that the rate of change of energy for this system is

$$-hC_D \ \underline{u_0}^2 - \underline{u_0}.\underline{u} + \underline{u}^2$$

which is negative definite. If we were to try to reduce this equation set to one equation in one variable we find that we cannot do it. This is because we are unable to replace $\underline{u_0}$ in the time derivatives of equation 5.7 with $\partial h/\partial t$ by using equations 5.9 and 5.10 without obtaining time derivatives of $\underline{u}$, which we cannot then eliminate.

We now consider an alternative way of including friction, namely,

$$D\,D\,D\partial h\,to \quad fc\,facos\,.f\,D\,D\partial h D\lambda \quad fcD\,f\partial\lambda D\,..u\,h\,w\,tn fv\,D\,cD \quad SD\,t$$

probably better to ask if there are any valid solutions to these equations which can give rise to a positive energy source. It is thus possible that this second system may be the better one to use, particularly as it could be considered as the more obvious of the two. This is because the first system used by Cullen is not the one obtained by simply using the Ekman velocity rather than the geostrophic wind in the geostrophic momentum approximation used to derive the equations. The system obtained that way is in fact this second system, for which the existence and uniqueness of solutions could be proved using the approach of Chapter 2 providing we can prove the outstanding results from Chapter 2. This is an area where more work may be useful.

ibliography

[1] H. H. Ahlberg, E. N. Nilson, J. L. Walsh. *The The*

[8] W. L. Briggs, *Multigrid tutorial.* SIAM 1987.

[9] E. Coddington and N. Levinson. *Theory of Ordinary ifferential Equations.* McGraw-Hill 1955.

[10] F. Castelli, R. L. Bras and K. A. Emanuel. *n analytic approach to the non-linear dynamics of moist frontogenesis.* J. Atmos. Sci. **50** pp 1504–1518, 1993.

[11] J. G. Charney. *The dynamics of long waves in a baroclinic current.* J. Meteor. **4** pp 135–163, 1947.

[12] J. G. Charney, R. Fjortoft and J. von Neumann. *Numerical integration of the barotropic vorticity equation.* Tellus, **2** pp 237–254, 1950.

[13] S. Chynoweth, D. Porter and M. J. Sewell. *The parabolic umbilic and atmospheric fronts.* Proc. R. Soc. Lond. **419** pp 337–362, 1988.

[14] M. J. P. Cullen. *Integrations of the primitive equations on a sphere using the finite element method.* Quart. J. Roy. Met. Soc. **100** pp 555–562, 1974.

[15] M. J. P. Cullen. *Implicit Finite- ifference Method for Modelling iscontinuous tmospheric Flows.* J. Comp. Phys. **81** pp 319–348, 1989.

[16] M. J. P. Cullen. *On the incorporation of atmospheric boundary layer effects into a balanced model.* Quart. J. Roy. Met. Soc. **115** pp 1109–1131, 1989.

[17] M. J. P. Cullen, S. Chynoweth and R. J. Purser. *On semi-geostrophic flow over synoptic scale topography.* Quart. J. Roy. Met. Soc. **113** pp 163–1806.2].

[19] M. J. P. Cullen, T. Davies and M. H. Mawson. *Conservative finite difference schemes for a unified forecast/climate model.* Unified Model Documentation Paper 10. Unpublished paper available from U.K. Meteorological Office.

[20] M. J. P. Cullen and R. J. Purser.

[29] J. Gary, S. McCormick and R. Sweet. *uccessive Over-Relaxation, Multigrid, and Preconditioned Conjugent Gradient lgorithms for solving a iffusion Problem on a Vector Computer.* Appl. Maths. and Comp. **13** pp 285–309, 1983.

[30] P. R. Gent and J. C. McWilliams. *Consistent balanced models in bounded and periodic domains.* Dyn. Atmos. Oceans **7** pp 67–93, 1983.

[31] P. R. Gent and J. C. McWilliams. *Regimes of validity for balanced models.* Dyn. Atmos. Oceans **7** pp 167–183, 1983.

[32] W. Hackbusch. *Multigrid methods and applications.* Springer-Verlag, Berlin, 1985.

[33] B. Haurwitz. *The motion of atmospheric disturbances on the spherical earth.* J. Marine Res. **3** pp 254–267, 1940.

[34] M. W. Holt. *emi-geostrophic moist frontogenesis in a Lagrangian model.* Dyn. Atmos. Oceans **14** pp463–481, 1990.

[35] M. W. Holt and A. J. Thorpe. *Localized forcing of slantwise motion at fronts.* Quart. J. Roy. Met. Soc. **117** pp 943–963, 1991.

[36] B. J. Hoskins. *The geostrophic momentum approximation and the semi-geostrophic equations.* J. Atmos. Sci. **32** pp 233–242, 1975.

[37] B. J. Hoskins. *tability of the Rossby-Haurwitz wave.* Quart. J. Roy. Meteor. Soc. **99**, pp 723–745, 1973.

[38] B. J. Hoskins and F. P. Bretherton. *tmospheric frontogenesis models: mathematical formulation and solution.* J. Atmos. Sci. **29** pp 11–37, 1972.

[39] B. J. Hoskins, M. E. McIntyre and A. W. Robertson. *On the use and significance of isentropic potential vorticity maps.* Quart. J. Roy. Meteor. Soc. **111** pp 877–946, 1985.

[40] J. Linden, B. Steckel and K. Stüben. *Parallel multigrid solution of the Navier-tokes equations on general 2- domains.* Parallel Computing **7**, 1988.

[41] P. Lynch and Xiang-Yu Huang. *Initialisation of the HIRL M model using a digital filter.* Mon. Wea. Rev. **120** pp 1019–1034, 1992.

[42] A. McDonald. *semi-LagrPar*

Monfl

[48] M. H. Mawson and M. J. P

[59] L. F. Richardson. *Weather prediction by numerical process.* Cambridge University Press, 236pp. 1922. Reprinted by Dover.

[60] C. A. Riegel and A. F. C. Bridger. *Fundamentals of atmospheric dynamics and hydrodynamics.* World Science 1992.

[61] A. Robert. *stable numerical integration scheme for the primitive meteorological equations.* Atmos. Ocean. **19** pp 35–46, 1981.

[62] G. Robinson. *Fluid dynamics in parallel using an unstructured mesh.* First International Conference on Parallel Processing for Computational Mechanics, Southampton, 1990.

[63] R. Salmon. *New equations for nearly geostrophic flow.* J. Fluid Mech. **153** pp 461–477, 1985.

[64] R. Salmon. *emigeostrophic theory as a dirac-bracket projection.* J. Fluid. Mech. **196** pp 345–358, 1988.

[65] R. Salmon. *What is potential vorticity ?* Woods Hole Oceanog. Inst. Tech. Rept., WHOI-93-24, pp 181–185, 1993.

[66] T. I. Seidman. *ome "Complexity" Issues for Ill-Posed Problems.* Inverse Problems in Partial Differential Equations. Edited by D. Colton, R. Ewing and W. Rundell, SIAM 1990.

[67] W. N. Shaw. *We*

[70] J. Smagorinsky. *Global atmospheric modelling and the numerical simulation*

[79] R. Wu and W. Blumen. *n analysis of Ekman boundary layer dynamics incorporating the geostrophic momentum approximation.* J. Atmos. Sci. **39** pp 1774–1782, 1982.

[80] J. A. Young. *theory for isallobaric flow in the planetary boundary layer.* J. Atmos. Sci. **30** pp 1584–1592, 1973.